Current Research in Parasitology & Vector-Borne Diseases 1 (2021) 100014

Contents lists available at ScienceDirect

Current Research in Parasitology & Vector-Borne Diseases

journal homepage: www.editorialmanager.com/crpvbd/default.aspx

Modeling the association between *Aedes aegypti* ovitrap egg counts, multi-scale remotely sensed environmental data and arboviral cases at Puntarenas, Costa Rica (2017–2018)

Luis Fernando Chaves [a,*], José Angel Valerín Cordero [b], Gabriela Delgado [c], Carlos Aguilar-Avendaño [c], Ezequías Maynes [c], José Manuel Gutiérrez Alvarado [c], Melissa Ramírez Rojas [a], Luis Mario Romero [d], Rodrigo Marín Rodríguez [a,c]

[a] *Vigilancia de la Salud, Ministerio de Salud, San José, San José, Apartado Postal 10123-1000, Costa Rica*
[b] *Coordinación Regional, Programa Nacional de Manejo Integrado de Vectores, Región Pacífico Central, Ministerio de Salud, Puntarenas, Puntarenas, Código Postal 60101, Costa Rica*
[c] *Oficina Central de Enlace, Programa Nacional de Manejo Integrado de Vectores, Ministerio de Salud, San José, San José, Apartado Postal 10123-1000, Costa Rica*
[d] *Departamento de Patología, Escuela de Medicina Veterinaria, Universidad Nacional, Heredia, Heredia, Apartado Postal 304-3000, Costa Rica*

ARTICLE INFO

Keywords:
Oviposition
MODIS
Landsat 8
Sentinel 2
Schmalhausen's law
Model selection
Synchrony
Syndemic arboviruses

ABSTRACT

Problems with vector surveillance are a major barrier for the effective control of vector-borne disease transmission through Latin America. Here, we present results from a 80-week longitudinal study where *Aedes aegypti* (L.) (Diptera: Culicidae) ovitraps were monitored weekly at 92 locations in Puntarenas, a coastal city in Costa Rica with syndemic Zika, chikungunya and dengue transmission. We used separate models to investigate the association of either *Ae. aegypti*-borne arboviral cases or *Ae. aegypti* egg counts with remotely sensed environmental variables. We also evaluated whether *Ae. aegypti*-borne arboviral cases were associated with *Ae. aegypti* egg counts. Using cross-correlation and time series modeling, we found that arboviral cases were not significantly associated with *Ae. aegypti* egg counts. Through model selection we found that cases had a non-linear response to multi-scale (1-km and 30-m resolution) measurements of temperature standard deviation (SD) with a lag of up to 4 weeks, while simultaneously increasing with finely-grained NDVI (30-m resolution). Meanwhile, median ovitrap *Ae. aegypti* egg counts increased, and respectively decreased, with temperature SD (1-km resolution) and EVI (30-m resolution) with a lag of 6 weeks. A synchrony analysis showed that egg counts had a travelling wave pattern, with synchrony showing cyclic changes with distance, a pattern not observed in remotely sensed data with 30-m and 10-m resolution. Spatially, using generalized additive models, we found that eggs were more abundant at locations with higher temperatures and where EVI was leptokurtic during the study period. Our results suggest that, in Puntarenas, remotely sensed environmental variables are associated with both *Ae. aegypti*-borne arbovirus transmission and *Ae. aegypti* egg counts from ovitraps.

1. Introduction

Pathogens transmitted by *Aedes aegypti* (L.) (Diptera: Culicidae) are a major health problem throughout Latin America and the Caribbean (Wallace et al., 2018). Dengue (San Martín et al., 2010; Perez et al., 2019), Zika (Colón-González et al., 2017) and chikungunya (Yactayo et al., 2016) have become syndemic through most of the region, and problems with vector surveillance and control seem to be a major driver for the impact of these diseases through Latin America (Fernández-Salas et al., 2015; Weaver et al., 2016) and elsewhere (Weaver & Reisen, 2010; Weaver et al., 2018). One tool that has proved highly efficient for the surveillance of *Ae. aegypti* is the systematic ovitrap sampling, which can be used for entomological surveillance (CENAPRECE, 2015), both to detect its presence (Baak-Baak et al., 2016; Ortega-Morales et al., 2018) and estimate its abundance (Tovar-Zamora et al., 2019). Ovitraps can also be used for mosquito population control (Ritchie et al., 2003, 2004; Barrera et al., 2014, 2017; Martin et al., 2019).

* Corresponding author.
E-mail address: lfchavs@gmail.com (L.F. Chaves).

https://doi.org/10.1016/j.crpvbd.2021.100014
Received 24 November 2020; Received in revised form 20 January 2021; Accepted 26 January 2021

In Costa Rica, dengue, chikungunya and Zika are the most common arboviruses affecting humans, and account for the highest vector-borne disease burden in the country, given their high case number, which is in the magnitude of thousands of annual cases (Soto-Garita et al., 2016; Vigilancia de la Salud, 2019). This case load is well above what is observed for other vector-borne diseases, such as cutaneous leishmaniasis, where annual cases amount to a few hundred (Chaves et al., 2008), or malaria, which is on the brink of elimination (Chaves et al., 2020a). In Costa Rica, dengue transmission has been traditionally located at low altitudes, on coastal regions from the Pacific and Caribbean basins (Mena et al., 2011). On the Pacific basin, the county of Puntarenas has experienced high transmission of *Ae. aegypti*-borne pathogens over recent decades. For example, a serological survey found over 90% of the people exposed to dengue virus (Lee-Lui et al., 2008). Moreover, Puntarenas county is regularly among the top 10% of counties reporting dengue cases in Costa Rica (Vigilancia de la Salud, 2019).

Aedes aegypti has a long history in Puntarenas and was documented to be present by 1920 (Alfaro, 1921; Serre, 1921) and the late part of the 1930s (Kumm et al., 1940). In 1961, the country was certified as free from *Ae. aegypti* as part of yellow fever eradication efforts (Soper, 1967), a status held until at least 1988 (Gubler, 1989). However, in 1993 local dengue transmission started, implying that *Ae. aegypti* was again present in Puntarenas (Sáenz et al., 1999). Recent studies have identified that key larval habitats of *Ae. aegypti* in Puntarenas include artificial discarded containers, but also water holding tanks, and other containers with active domestic use (Troyo et al., 2009; Marín Rodríguez & Díaz Ríos, 2012). A couple of studies have described insecticide resistance patterns in *Ae. aegypti* from Puntarenas. Bisset et al. (2013) reported resistance to the pyrethroid deltamethrin and to the organophosphate temephos used for larval control. Zardkoohi et al. (2020) confirmed the resistance to deltamethrin, and the emergence of resistance to the pyrethroid cypermethrin, linking pyrethroid resistance to the co-occurrence of the V1016I and F1534C *kdr* mutations in the voltage-gated sodium channel gene.

Several studies have linked weather changes with both *Ae. aegypti* abundance and arboviral pathogen transmission (Scott et al., 2000; Johansson et al., 2009; Chaves, 2017a; Reinhold et al., 2018). However, no attempt has been made at linking temporal changes in *Ae. aegypti*-borne arboviral transmission, and *Ae. aegypti* abundance, with weather variables at Puntarenas, which is, and has historically been, a major focus for dengue transmission in Costa Rica. This potential association is particularly important because a global meta-analysis found limited evidence for dengue transmission prediction based on data from entomological surveys of *Ae. aegypti* aquatic stages (Bowman et al., 2014). One major problem to test if dengue transmission was associated with entomological indicators was the lack of a spatially standardized sampling (Bowman et al., 2014), which is more feasible with ovitraps (CENAPRECE, 2015). In Costa Rica, ovitraps have been successfully used to survey mosquito biodiversity (Chaverri et al., 2018) and to study mosquito population dynamics (Romero et al., 2019). Moreover, the Costa Rican National programme for integrated vector management started to use ovitraps to guide vector control in 2017, as done elsewhere in Latin America (Regis et al., 2008; CENAPRECE, 2015; PAHO, 2017). All these conditions make Puntarenas an ideal site to test if arboviral cases can be associated with *Ae. aegypti* egg counts from ovitraps.

Here, we present the results of an 80-week longitudinal study where weekly observations on the number of eggs at 92 ovitrap locations were recorded between 2017 and 2018. We tested whether remotely sensed environmental data and *Ae. aegypti* egg counts from ovitraps can be associated with arboviral transmission in Puntarenas, a city on the Pacific Coast of Costa Rica. Additionally, we also tested whether egg counts were associated with remotely sensed environmental variables.

For our analysis, we employed satellite images with different resolution. Specifically, we included Sentinel 2 (10 m resolution), Landsat 8 (30 m) and MODIS (250 m and 1 km). We used several temporal, spatio-temporal and spatial modelling techniques. We started by (i) performing an ancillary analysis comparing land surface temperature estimates obtained with MODIS images for the Puntarenas city area, where cases were recorded, with estimates based on Landsat 8 images for the Puntarenas peninsula area, the subsection of Puntarenas city where most of the transmission is assumed to occur (Marín Rodríguez & Díaz Ríos, 2012).

We then developed (ii) time series models to assess the association between the remotely sensed environmental variables with *Ae. aegypti* egg counts and *Ae. aegypti*-borne arboviral cases. We specifically employed seasonal autoregressive (SAR) models given their ease for fitting and interpretation (Chaves & Pascual, 2007). Among other things, these models allow testing for the significance of environmental variables at time lags whose association with the studied time series is not an artifact of a similar, but unrelated, seasonality (Priestley, 1988). These models allow to evaluate if the arboviral cases were associated with egg counts and remotely sensed environmental variables at different time lags. This analytic framework was also used to assess the association between egg counts and remotely sensed environmental variables at different lags.

We also performed (iii) a synchrony analysis of *Ae. aegypti* egg counts and the remotely sensed environmental variables based on Landsat 8 and Sentinel 2 images. This is an innovative analysis to study spatio-temporal patterns in mosquito oviposition, which we have previously used to study mosquito larval (Chaves et al., 2020b) and adult (Chaves, 2017b) abundance patterns. Briefly, a synchrony analysis shows the degree of concerted fluctuation between values of a studied variable, egg counts in this study, as a function of the distance separating the sampling locations (Chaves et al., 2013). This analysis allows to test if the correlations between egg counts are synchronous, i.e. not changing with distance. Alternatively, the correlations can decay with distance as expected under dispersal limitation, or have a fluctuating sign, changing from positive to negative, with distance, as expected when dispersal occur in traveling waves (Ranta et al., 2006). Thus, the synchrony analysis provides a description of the type of spatial heterogeneity in oviposition, measured through time. The obtained oviposition synchrony can also be compared with the synchrony in environmental data to establish a dependence of the former on the latter (Chaves et al., 2013).

We finished by performing a (iv) spatial analysis of the mean number of *Ae. aegypti* eggs at each sampled location with average values for the remotely sensed environmental variables, based on Landsat 8 and Sentinel 2 images, at the pixels where traps were located. For this analysis, we employed generalized additive models. This modelling framework enables to easily incorporate nonlinearities in the association between variables (Faraway, 2006). This analysis allowed to test if average egg counts were associated with average environmental conditions estimated from finely-grained (30 m and 10 m) remotely sensed data.

2. Materials and methods

2.1. Study site

Our study was carried out in Puntarenas city (9°58′34.50″N, 84°50′18.10″W), the largest city on the Pacific coast of Costa Rica (Fig. 1), capital of Puntarenas county and Puntarenas province. The urban area of Puntarenas city is formed by Puntarenas, Chacarita, Barrancas, El Roble and Pitahaya districts (Fig. 1). The city has a population of 81,187 inhabitants, according to the last census (2011), and 193.98 km^2 of area, for a population density of 418 inhabitants/km^2 (INEC, 2012). Puntarenas peninsula, the peninsular part of Puntarenas district (Fig. 1), concentrates government, education and commercial activities of Puntarenas city (Villanueva, 2009). Bus and ferry terminals that serve as transportation hubs for Puntarenas city, Puntarenas county and the Pacific basin of Costa Rica are also located in the Puntarenas peninsula (Chen et al., 2017).

Puntarenas city has a marked seasonal climatic pattern with a dry season from December to April, and a rainy season over the rest of the

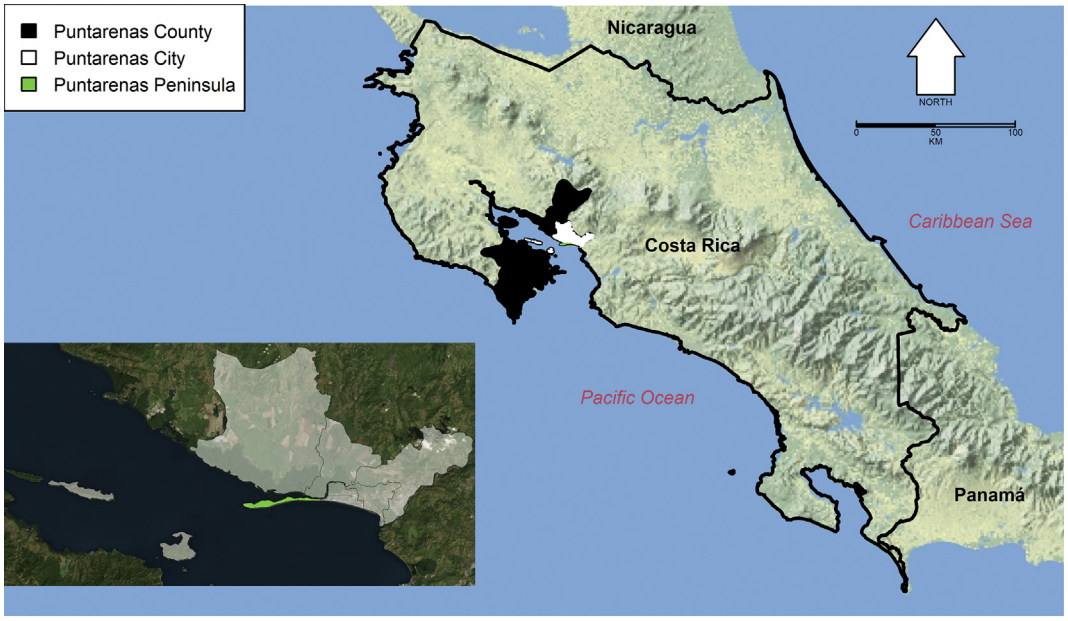

Fig. 1 Map of Costa Rica and Puntarenas city. The map highlights the location of Puntarenas county and the inset map highlights the urban area of Puntarenas city and the Puntarenas peninsula part of Puntarenas district. The base image for the main map is from a public domain map from the US National Park Service (USNPS, 2020), while the inset base image is courtesy of Google maps

year (World Meteorological Organization, 2020). The average annual total cumulative rainfall is 1,600 mm, while temperature has an annual average of 32.8 °C, which is about 2.1 °C hotter during the dry season than the rainy season (World Meteorological Organization, 2020).

2.2. Mosquito sampling

Mosquitoes were sampled using ovitraps made with PVC plastic. The ovitraps have a cylindrical shape (diameter of 11 cm and height of 14 cm), with a closed and an open end (Fig. 2A) and were donated by the Mexican Government through the Center for Infectious Disease Control and Prevention (CENAPRECE), a branch of Mexico's Secretary of Health. The ovitraps have two 5 mm in diameter openings 8 cm above the closed end, thus having a water holding volume of 750 ml. Ovitraps were set using Scott® paper towels (Kimberly Clark Co., Neenah, WI, USA), which were placed around the internal side of the ovitrap. Following the recommendations from CENAPRECE (2015) we filled the ovitraps with 750 ml of tap water. This water came from the city water distribution network, where chlorine concentrations are strictly monitored and fluctuate between 0.3 and 0.6 mg/l (Marín Mena, 2007). The paper towels

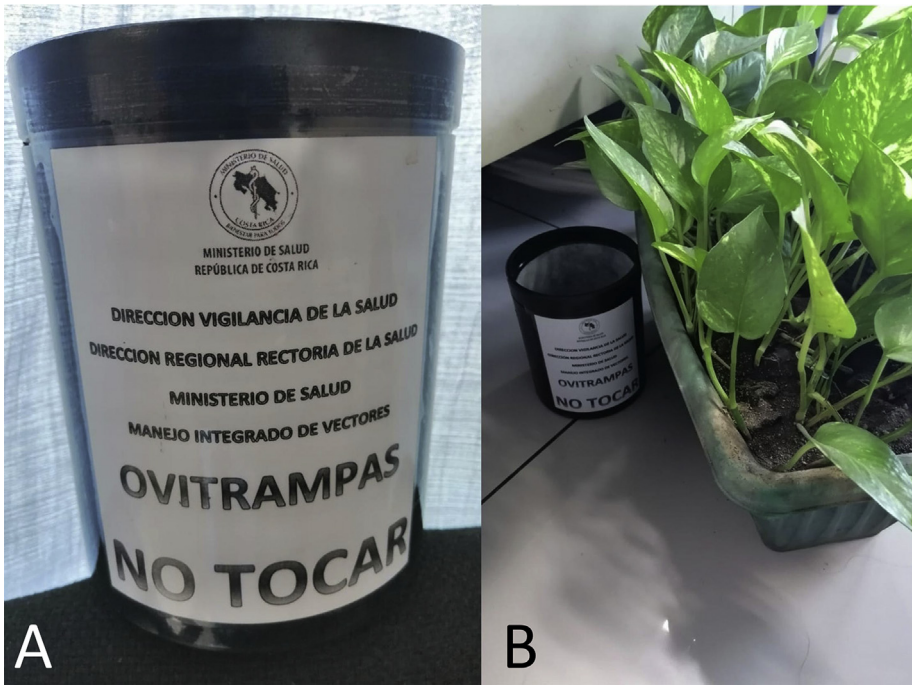

Fig. 2 Ovitraps. **A** Ovitrap label indicating its use for dengue vector surveillance and providing contact information for the Programa de Manejo Integrado de Vectores of Costa Rica's Ministry of Health. **B** Field deployment of an ovitrap, next to a plant pot, a common larval habitat for *Aedes aegypti* in Puntarenas, Costa Rica

were added to sample *Ae. aegypti* eggs, given the oviposition behavior of this species which places eggs on surfaces above the water line (Chadee & Corbet, 1987). Traps were labeled (Fig. 2A) and deployed (Fig. 2B) following a protocol developed by the CENAPRECE (2015).

A total of 92 traps were deployed on April 17th, 2017 (epidemiological week 16) through the Puntarenas peninsula (Fig. 3). Both the water and the paper towels were replaced every Monday from epidemiological week 17 of 2017 (April 24th 2017) to epidemiological week 44 of 2018 (October 29th 2018). This was done to avoid biases in mosquito sampling related to ovitrap water age and/or conspecific presence (Chadee, 2009). Ovitraps were placed inside the houses ($n = 90$) or outside the houses but within the household space, e.g. the backyard, specifically an area outside the houses where a sink for washing clothes ("pila" in the Spanish of Costa Rica) is traditionally located ($n = 2$). Ovitraps were placed next to the walls defining the residential premises, i.e. within approximately within one meter from the wall (within 1 m), in places selected by the homeowners, but restricted to the first floor of multi-story buildings. Traps were deployed following CENAPRECE (2015) recommendations, i.e. a maximum of 4 ovitraps were deployed by residential block, "manzana" in Spanish, trying to ensure a minimal distance between any pair of traps was 20 m, something done because of the finely-grained nature of *Ae. aegypti* oviposition (Harrington et al., 2008). Homeowners were asked for consent to place the ovitraps in their households as part of efforts for arbovirus transmission surveillance.

In light of insights about dengue transmission in public spaces with a high turnover of visitants and human movement (Stoddard et al., 2009; Arunachalam et al., 2010; Smith et al., 2014), ovitraps were located within the Puntarenas peninsula. This decision was made given that Puntarenas peninsula serves as a hub for human movement within Puntarenas city (Chen et al., 2017) and because previous studies have shown persistent mosquito infestations in the area (Marín Rodríguez & Díaz Ríos, 2012) suggesting that the peninsula is a place where most *Ae. aegypti*-borne arboviruses are transmitted among inhabitants of the larger Puntarenas city (Marín Rodríguez & Díaz Ríos, 2012).

Ovitraps were georeferenced using the recorded address for each ovitrap with Google maps. Paper towels were individually transported inside identified medium sized (17.7 × 18.8 cm) freezer Ziploc® bags (SC Johnson Co., San Mateo Otzacatipan, México) to the Coordinación Regional of Programa Nacional de Manejo Integrado de Vectores in Puntarenas, Costa Rica, where eggs were counted under a 10× dissecting microscope. The counting was carried out under a dissecting microscope to ensure that eggs of *Limatus* spp., if present, were separated from *Aedes* spp. eggs, given the striking morphological differences between these two mosquito genera and the potential colonization of ovitraps by *Limatus durhami* Theobald, a species present in the study area (Calderón-Arguedas et al., 2009), and considering that *Limatus* spp. also oviposit on surfaces above the water line (Santos Neto & Azevedo Marques, 1996; Ceretti-Júnior et al., 2014; Carvalho et al., 2017). Briefly, *Limatus* spp. eggs have a shape similar to a boomerang (or elongated rhombus), as opposed to the elongated elliptical shape of *Aedes* spp. eggs (Santos Neto & Azevedo Marques, 1996). Other species in the studied area (Vargas, 1961; Calderón-Arguedas et al., 2009) that could potentially colonize ovitraps included *Culex* spp. and *Uranotaenia* spp., both of which oviposit in rafts and whose eggs are projected into the water surface (Harbach & Knight, 1978; Day, 2016), and *Toxorhynchites* spp., which oviposit single eggs, that are significantly larger than eggs from other mosquito genera and that are also projected into the water surface (Chadee et al., 1987). For further mosquito identification quality control, each week up to 100 eggs from 3 randomly chosen traps were allowed to hatch to verify the identity of the species collected. Throughout the study, eggs from each ovitrap location were checked at least once; all samples collected belonging to *Ae. aegypti*. In addition, Puntarenas peninsula is an area without current or historical records for the presence of *Aedes albopictus* (Skuse) (Futami et al., 2015). During this study, we did not find *Limatus* spp. eggs while examining and counting sampled eggs under the dissecting microscope.

2.3. Arboviral disease data

Weekly counts for Zika, dengue and chikungunya cases from Puntarenas county, for all the weeks of 2017 and 2018, were obtained from the weekly epidemiological bulletins published by the epidemic surveillance division (Vigilancia de la Salud) from Costa Rica's Ministry of Health which are publicly available at: https://www.ministeriodesalud.go.cr/index.php/vigilancia-de-la-salud/boletines/enfermedades-de-transmision-vectorial-2017. These case counts include all clinically diagnosed dengue cases, of which a variable proportion, ensuring all presumed transmission clusters are sampled, are confirmed by PCR and/or serological methods by the Costa Rican National Reference Laboratory for viral infections (González Elizondo, 2018). All Zika and chikungunya cases are confirmed by laboratory methods (PCR and/or serology), before being consolidated and reported by the epidemic surveillance division at Costa Rica's Ministry of Health. Independently of the moment when the final diagnostic is performed, cases are recorded for the week individuals attend health facilities with symptoms of an arboviral infection.

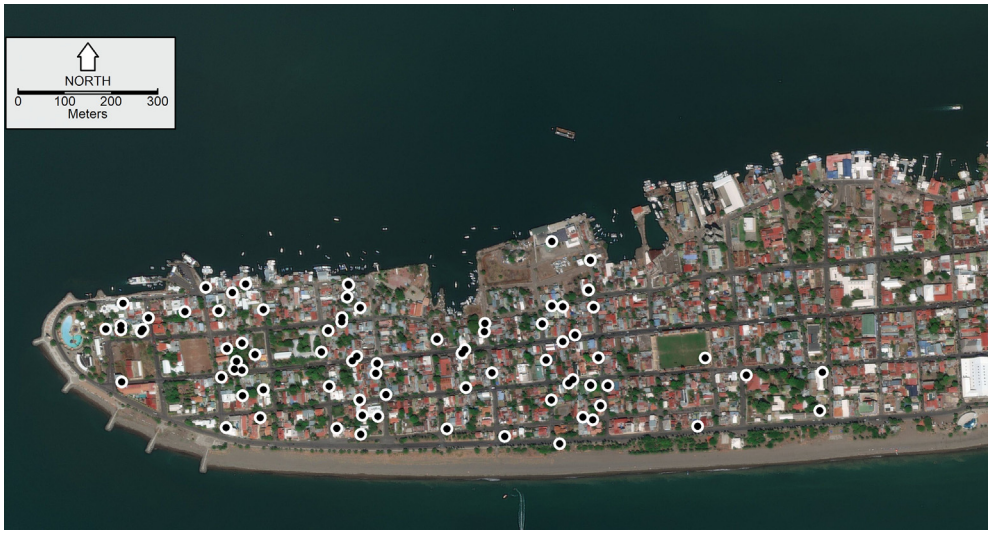

Fig. 3 Ovitrap sampling locations. Ovitraps are indicated by dots on the map. The location of only 83 of 92 the ovitraps are shown since 9 records had ambiguous addresses that could not be found using Google maps. The base image is courtesy of Google maps

2.4. Remotely sensed data (temperature and vegetation growth)

We downloaded daily images for land surface temperature and emissivity (LST&E) with a spatial resolution of 1 km (MOD1101, Version 6) based on Moderate Resolution Imaging Spectroradiometer (MODIS) images (Wan et al., 2015). The images were re-scaled by multiplying each pixel by a factor of 0.02, and the resulting temperatures were transformed from °K to °C by subtracting 273 (Wan et al., 2015). Downloaded MODIS images can be seen in the supplementary online Video S1. We generated Landsat 8 land surface temperature images with a spatial resolution of 30 m using a script for online use with Google Earth Engine (Ermida et al., 2020). Downloaded Landsat 8 images can be seen in the supplementary online Video S2 and were available every 8 days.

Supplementary videos related to this article can be found at https://doi.org/10.1016/j.crpvbd.2021.100014

We also downloaded images for the Normalized Difference Vegetation Index (NDVI) and Enhanced Vegetation Index (EVI), both of which are considered proxies for vegetation growth (Pettorelli et al., 2005) and have been extensively used to study the ecology of mosquitoes (Hurtado et al., 2018b; Chaves et al., 2019; Poh et al., 2019; Rigg et al., 2019; Nguyen et al., 2020; Chaves & Friberg, 2021) and other insect vectors (Kitron et al., 1996). The images for vegetation indices were downloaded for the multiple spatial scales encompassed by MODIS, Landsat 8 and Sentinel 2. The MODIS NDVI and EVI images were processed every 16 days, have a spatial resolution of 250 m (MOD13Q1, version 6 and MYD13Q1, version 6) and are collected by Terra and Aqua satellites (Didan, 2015a, b). These images were re-scaled by dividing the values of each pixel by 10,000, thus obtaining normalized values that range between −1 and 1 (Pettorelli et al., 2005). We used data from Terra (MOD13Q1) and Aqua (MYD13Q1) satellites, to increase the number of observations used to estimate environmental time series. This also allowed us to increase the frequency of observations to every 8 days provided the delay between the images from each satellite for the study site.

We also used information from the red (RED, band 4) and near infrared (NIR, band 5) Landsat 8 bands, with a resolution of 30 m, downloaded with the Landsat 8 land surface temperature to estimate NDVI using the following equation (Vermote et al., 2016):

$$NDVI = \frac{(NIR - RED)}{(NIR + RED)} \quad (1)$$

Adding information from the Landsat 8 blue band (BLUE, band 2), we estimated EVI using the following equation (Vermote et al., 2016):

$$EVI = 2.5^{*}\frac{(NIR - RED)}{(NIR + 6^{*}RED - 7.5^{*}BLUE + 1)} \quad (2)$$

The resulting images were used to estimate Landsat 8-based NDVI and EVI. Equations (1) and (2) were also used to estimate NDVI and EVI using top of the atmosphere Sentinel 2 images, which have a resolution of 10 m and where BLUE is band 2, RED is band 4 and NIR is band 8 (Drusch et al., 2012). Sentinel 2 images for the study period were processed using the Google Earth Engine to remove pixels covered by clouds or whose values exceeded the theoretical bounding values of −1 to 1 (ESA, 2015). Downloaded Sentinel 2 images can be seen in the supplementary online Video S3, and were available every 3.4 ± 2.0 days.

Supplementary videos related to this article can be found at https://doi.org/10.1016/j.crpvbd.2021.100014

To generate MODIS-based temperature, NDVI and EVI time series, each image was cropped using a polygon from the joint area of the 5 districts conforming the urban area of Puntarenas (Fig. 1) using the package "*raster*" in R (Brunsdon & Comber, 2015) and mean values were estimated for the selected pixels containing information. We repeated this process for the Landsat 8-based temperature images, and Landsat 8- and Sentinel 2-based NDVI and EVI images, but cropping only the area corresponding to the Puntarenas peninsula (Fig. 1). The difference in the cropped areas was due to three main reasons: (i) over 90% of the arboviral cases occur in the Puntarenas city area of Puntarenas county, with over 80% of the cases linked with activities in the Puntarenas peninsula area (Vigilancia de la Salud, 2019) and such area is more easily covered by the lower resolution MODIS images; (ii) traps were deployed in the Puntarenas peninsula area, at distances where the spatial resolution of Landsat 8 and Sentinel 2 images is more likely to detect differences in the local environments were traps were located (which had a mean ± standard deviation (SD) of 495 ± 311 m, Supplementary Fig. S1); and (iii) having multi-scale spatial images allowed us to test the hypothesis that both local and regional environmental factors might be involved in arbovirus transmission and *Ae. aegypti* oviposition. In addition, for MODIS and Landsat 8 temperature images we estimated time series for the SD and kurtosis, respectively, in the Puntarenas city and peninsula area, given the possibility that arboviral cases and egg counts are sensitive to patterns of variability in the environment, as predicted by Schmalhausen's law, the biological principle stating that organisms follow both the mean and higher order moments, i.e. SD and kurtosis, of environmental variation (Chaves, 2017a).

The resulting time series were then smoothed using the loess algorithm for local polynomial regression fitting (Cleveland & Devlin, 1988) by performing a regression of the estimated temperature, NDVI or EVI as a function of the day when the images were acquired by the satellites. For the loess, we employed a neighborhood size of 10% of the data and second-degree polynomials.

The resulting smoothed time series were then used to obtain weekly estimates of NDVI and EVI, extrapolating values to the Monday of each week in the case of NDVI and EVI from MODIS, Landsat 8 and Sentinel 2 images, and also for land surface temperatures, including mean, SD and kurtosis from Landsat 8 images. However, for MODIS-based temperatures, we estimated weekly average, SD and kurtosis from Tuesday to Monday, using the daily temperature time series.

All MODIS and Landsat 8 images were courtesy of the NASA Land Processes Distributed Active Archive Center (LP DAAC) and the United States Geological Survey (USGS)/Earth Resources Observation and Science (EROS) Center (Sioux Falls, South Dakota). Copernicus Sentinel 2 data were processed, and provided free of charge, by the European Space Agency (ESA). All MODIS images were downloaded from the LP DAAC server (NASA, 2018) using the package *MODIStsp* in R (Busetto & Ranghetti, 2016). Landsat 8 and Sentinel 2 images were retrieved from the Google Earth Engine Dataset Catalog (Google, 2020).

2.5. Statistical analysis

Our statistical analysis had four main components.

2.5.1. Comparison of land surface temperature (LST) time series estimates with MODIS and Landsat 8 images

We examined LST time series estimated with MODIS (Supplementary Fig. S2A) and Landsat 8 (Supplementary Fig. S2B) using the Pearson's correlation coefficient (Zar, 1998). We also compared MODIS and Landsat 8 data examining their coefficient of variation (CV). The CV, formally defined as the ratio between the SD and the mean of a variable (Stearns, 1981), was estimated for each observation in the MODIS (Supplementary Fig. S2C) and Landsat 8 (Supplementary Fig. S2D) time series. Then we assessed any potential bias in the estimation of time series observations related to the number of available pixels by performing a linear regression of the LST CV as a function of the number of pixels used to estimate LST. We used MODIS images for the Puntarenas city area (Supplementary Fig. S2E) and Landsat 8 images (Supplementary Fig. S2F) for the Puntarenas peninsula area when estimating the regressions.

2.5.2. Time series modeling

We studied the association between *Ae. aegypti*-borne arboviruses (Zika, chikungunya and dengue) and *Ae. aegypti* egg counts and remotely

sensed environmental variables using the general framework of seasonal autoregressive (SAR) models (Shumway & Stoffer, 2011). SAR models have the general form:

$$X_t = \mu + \sum_{j=1}^{lmax} \varphi_j (X_{t-j} - \mu) + \sum_{s>lmax}^{smax} \varphi_s (X_{t-s} - \mu) - \sum_{j=1}^{lmax} \sum_{s>lmax}^{smax} \varphi_j \varphi_s (X_{t-j-s} - \mu) + \sum_{i=1}^{k} \beta_i Cov(i)_{t-m} + \varepsilon_t \quad (3)$$

where X_t is the focal variable, i.e., arboviral cases or mean number of eggs in this study, observed at time *t*, X_t is a function of itself at time *t-j*, and at time *t-s*, where *j* and *s* are the time lags for the "autoregressive" and "seasonal" parameters (φ_j and φ_s, respectively) that account for autoregressive and cyclical patterns in the time series of the focal variable studied, and *Cov(i)* indicates covariates, which are related to the focal variable under study according to parameters β_i. The SAR models can have any *k* number of covariates, as long as this number is shorter than the time series length, minus the number of seasonal and autoregressive parameters plus one, μ is the mean of the time series, and ε_t is the error, which is assumed to be normal, independent and identically distributed (Shumway & Stoffer, 2011). To develop SAR models, we started by the identification of the maximum time lags for the autoregressive and seasonal components of the model. For lag identification we employed autocorrelation (ACF) and partial autocorrelation (PACF) functions which show the correlation of time series observations at different time lags considering, respectively, the full time series or only consecutive lags (Hoshi et al., 2014). Based on information from these functions, a null SAR model was fitted and used to pre-whiten time series of covariates whose association is then evaluated by examining cross-correlation functions (CCFs) between the covariate time series and the focal time series. This analysis allows the identification of lags at which covariates are correlated with the studied variables. Pre-whitening was used to avoid the spurious identification of significant lags of association that emerge from time series having similar autocorrelation structures (Hoshi et al., 2017).

Models for the weekly combined case count of dengue, chikungunya and Zika considered as potential covariates the median, the SD and kurtosis of weekly collected eggs across all ovitraps, the mean of remotely sensed temperature, NDVI and EVI at the different spatial resolutions considered in this study. We also studied the median number of weekly collected eggs as a function of the mean of remotely sensed temperature, NDVI and EVI at the different spatial resolutions considered in this study. In both cases we considered the MODIS-based time series estimated for the whole Puntarenas city and the Landsat 8- and Sentinel 2-based time series estimated for the Puntarenas peninsula. This was done to test if environmental conditions specific to the area where most transmission is assumed to occur, i.e., the Puntarenas peninsula, were associated with transmission recorded for the larger Puntarenas city area in models for arboviral cases. Similarly, in models for *Ae. aegypti* egg counts we considered the MODIS-based environmental time series for the Puntarenas city area to test if environmental phenomena occurring at larger spatial scales could influence *Ae. aegypti* oviposition dynamics recorded in the Puntarenas peninsula.

When fitting the models, all selected covariates were demeaned to ease their interpretation in terms of changes above or below their means (Chaves et al., 2018). We selected the best models through the minimization of the Akaike Information Criterion (AIC), a metric that trades-off model goodness-of-fit and parameter number, employing a strategy of backward elimination, where models are simplified by comparing "nested" models with the same number of parameters that are not significantly different from the "parent" model that considered all variables that are left out in each of the simplified "nested" models (Chaves, 2016; Chaves & Moji, 2018), or until there were no significant differences through a Chi-square likelihood ratio test between the model minimizing AIC and simplified versions of such model (Chaves et al., 2019).

2.5.3. Synchrony analysis

We performed a synchrony analysis for *Ae. aegypti* oviposition and environmental variables estimated with Landsat 8 and Sentinel 2 images. This analysis was carried out to understand if concerted fluctuations in eggs/ovitrap during the study period followed similar changes in temperature and the vegetation indices that we studied. For the analysis, we employed a Mantel correlogram with inference based on a Monte Carlo test, whose null hypothesis is that synchrony across the range of distances separating sampling locations is equal to a global average, unless more extreme (Chaves, 2017b; Chaves et al., 2020b). For the analysis, we only considered up to 50% of the spatial extent of the data to avoid spurious results at long distances due to small sample size (Gouhier & Guichard, 2014), but estimated regional synchrony considering samples from all the georeferenced ovitraps that had, at most, one missing observation. To estimate the synchrony, we used the time series from the 44 ovitrap locations that did not have ($n = 27$) or had at most one missing observation ($n = 17$), which were inputted by taking the average of the two immediate observations, i.e. one time step before and after the missing observation, in order to increase the power for statistical inference (Gouhier & Guichard, 2014). We also estimated synchrony for environmental variables at the pixels that contained the ovitraps considered in the oviposition synchrony analysis. For this we extracted Land Surface Temperature (LST), NDVI and EVI data from Landsat 8 images, and NDVI and EVI data from Sentinel 2 images, at the pixels containing the 44 ovitraps used for the *Ae. aegypti* oviposition synchrony analysis. We inputted missing values for the resulting environmental time series following the procedure described in the time series modeling section. The 44 ovitraps used for this analysis did not include any of the two ovitraps placed outside the houses.

2.5.4. Spatial analysis

We tested whether mean number of *Ae. aegypti* egg counts at georeferenced ovitraps ($n = 81$, after excluding two locations whose remotely sense data was defective and nine that were impossible to be georeferenced, among which were the two placed outside the housing premises) were correlated with Landsat 8 (LST, NDVI, EVI) and Sentinel 2 (NDVI and EVI) remotely sensed data. We employed a linear regression described by the following equation:

$$Y_i = \mu + \sum_{j=1}^{k} \beta_j Cov(j)_i + \varepsilon_i \quad (4)$$

where Y_i is the mean number of *Ae. aegypti* eggs, through the study period, at ovitrap location *i*, *Cov(j)* indicates the mean of remotely sensed environmental covariates, which are related to the mean number of *Ae. aegypti* eggs according to parameters β_j, μ is the intercept, and ε_i is the error, which is assumed to be normal, independent and identically distributed (Faraway, 2004). Given that observations used to estimate the mean number of *Ae. aegypti* eggs at the ovitrap locations were not homogeneous during the study period, as a few traps were vandalized or contents accidently removed by household residents, we used error weights proportional to the number of trap-weeks used to estimate the means to accurately represent sampling effort during parameter estimation (Faraway, 2004). We then proceeded with model selection based on the minimization of the AIC, following the same steps already described for the time series models. We tested the best model for nonlinearities in the association with the selected covariates, and if any of the associations was non-linear, we proceeded with fitting a generalized additive model (Venables & Ripley, 2002) that used a smoothed function for the covariates whose association with the mean number of *Ae. aegypti* eggs was nonlinear. For the generalized additive model, we also used error weights proportional to the sampling effort at each ovitrap location.

Finally, we performed a Moran's I test on the best model residuals, a test with a null hypothesis that a variable is spatially independent (Brunsdon & Comber, 2015). For the Moran's I test we generated a spatial weights matrix linking ovitrap sampling locations within a

distance of 145 m, the largest minimum distance between any two ovitrap sampling locations. Once neighbors were identified, weights were made proportional to the number of neighbors for each sampling location (Brunsdon & Comber, 2015).

3. Results

3.1. Data summary statistics

A total of 381 cases of *Ae. aegypti*-borne arbovirus cases were recorded in Puntarenas county during the ovitrap monitoring period, i.e. from epidemiological week 17 of 2017 to epidemiological week 44 of 2018 (Fig. 4A). Of these, 11 were Zika infections, 19 were chikungunya infections and the remaining 351 cases were due to dengue infections (Fig. 4A). During the study period we counted a total of 291,369 *Ae. aegypti* eggs, over a total sampling effort of 7,360 ovitrap weeks. A total of 278 times (3.78% of the total sampling effort), we were unable to collect the paper towels with eggs from ovitraps due to diverse reasons, mainly accidental disturbances from residents, and very few instances of vandalism (only 5 ovitraps needed to be replaced during the study duration). Ovitraps had no eggs 39.56% of the times they were sampled, i.e. 2,912 times, with a weekly average (±SD) of ovitraps without eggs of 36.40 ± 10.91, weekly ranging from 14 to 62 ovitraps without eggs across the studied period. The average number of eggs (±SD) per ovitrap/week was 41.14 ± 75.94 with weekly trap counts ranging from 0 to 1,000 eggs (Fig. 4B). Raw data for individual ovitraps are presented in Supplementary Fig. S3. In general, the mean number of eggs for ovitraps was larger than the median, indicating oviposition was clustered at few ovitrap locations during the study period (Fig. 4B). The SD (Fig. 4C) and kurtosis (Fig. 4D) of eggs/ovitrap/week had regular peaks during the study period, which did not seem to coincide with peaks in arbovirus transmission (Fig. 4A) or egg counts (Fig. 4B).

3.2. Comparison of land surface temperature (LST) time series estimates with MODIS and Landsat 8 images and remotely sensed data seasonality

MODIS and Landsat 8-based Land Surface Temperature showed a clear seasonal pattern where temperature peaks were observed during the dry season of Puntarenas, weeks 1 to 16 of 2018 (Fig. 5A, raw MODIS and Landsat 8 data presented, respectively, in Supplementary Figs. S2A and S2B). These time series had a low CV (around 7%) for both MODIS (Supplementary Fig. S2C) and Landsat 8 (Supplementary Fig. S2D), meaning that pixel had a variability of up to 0.7 °C for each 10 °C of mean temperature in the areas over which the MODIS (Puntarenas city) and Landsat 8 (Puntarenas peninsula) time series were estimated. The estimates in the time series also had a very low sensitivity to the number of pixels considered for area estimations. Estimates, on average, only decreased on the order of 10^{-5} for MODIS (Supplementary Fig. S2E) and 10^{-6} for Landsat 8 (Supplementary Fig. S2F) for each pixel not considered on the area estimations. Interestingly, both time series, land surface temperature from MODIS and Landsat 8, were highly correlated (Pearson's $\hat{r} = 0.734$) despite the difference in resolution and areas over where these temperature time series were estimated. The MODIS-based temperature SD time series (Supplementary Fig. S4A) had a seasonal pattern different to its mean value, as the SD peaked during the dry season of Puntarenas. However, no clear patterns were observed for the MODIS-based temperature kurtosis time series (Supplementary Fig. S4B) which seemed to increase randomly, becoming more leptokurtic, i.e. with high

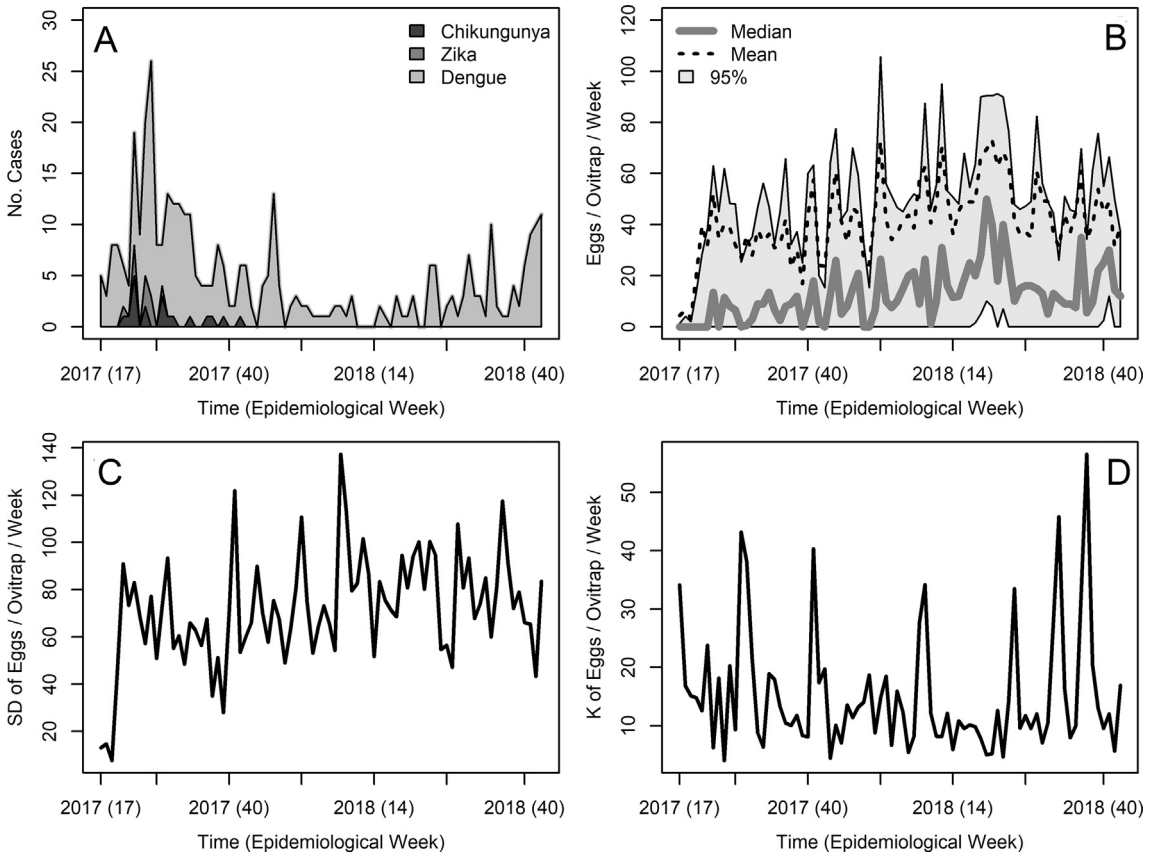

Fig. 4 Arboviral cases and mosquito time series. **A** Weekly counts of *Aedes aegypti*-borne arboviral cases in Puntarenas County. **B** Weekly distribution of *Ae. aegypti* egg counts across the ovitrap sampling locations. **C** Weekly standard deviation (SD) of *Ae. aegypti* egg counts across the ovitrap sampling locations. **D** Weekly kurtosis (K) of *Ae. aegypti* egg counts across the ovitrap sampling locations. Raw data including individual time series for each ovitrap sampling location are presented in Supplementary Fig. S3 at the journal website. See the inset legends for further details

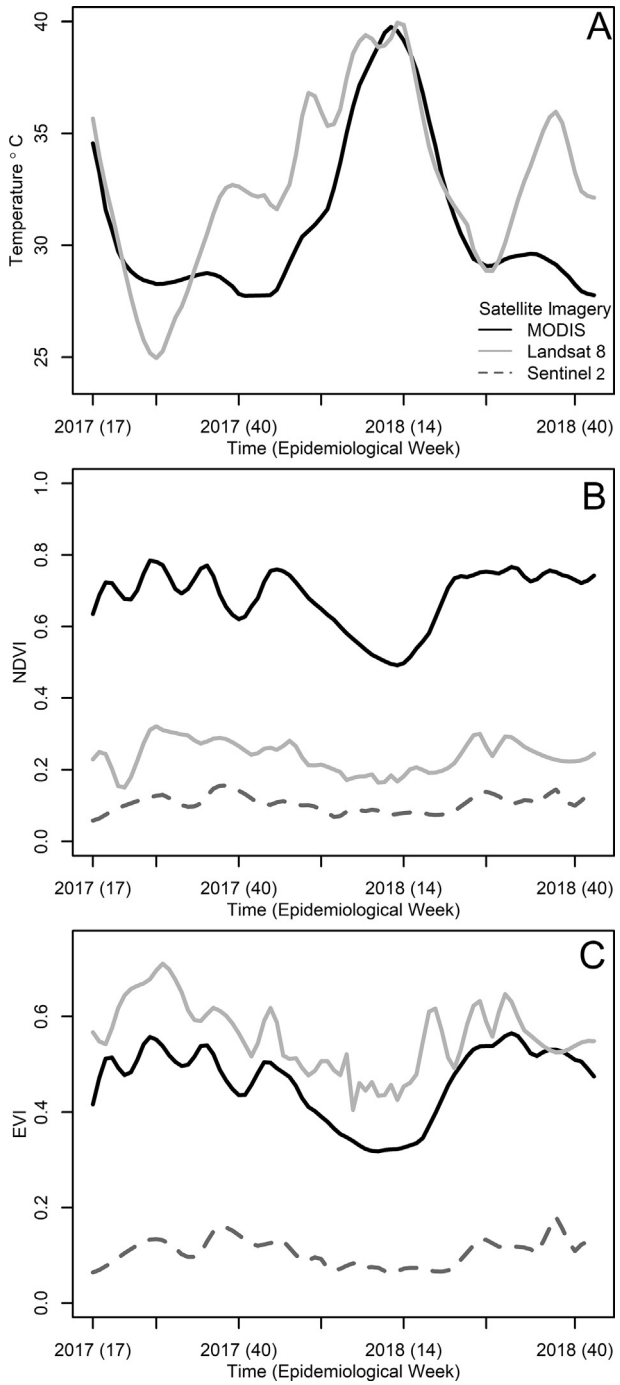

Fig. 5 Remotely sensed environmental time series. **A** Weekly mean land surface temperature derived from satellite images. **B** Weekly NDVI derived from satellite images. **C** Weekly EVI derived from satellite images. Temperature data originate from daily MODIS images, and Landsat 8 images collected every 8 days. NDVI and EVI time series also included Sentinel 2 data, which were collected every 3.4 ± 2.0 days (mean $\pm$ SD). For guidance, please refer to the inset legend of panel **A**. Raw and weekly smoothed data used to estimate these time series are presented in Supplementary Fig. S2 for MODIS and Landsat 8 land surface temperature, and raw data for the NDVI and EVI, derived from MODIS, Landsat 8 and Sentinel 2 are provided in Supplementary Fig. S5

kurtosis meaning temperature was more variable towards the extremes than around the mean of the distribution presented in Fig. 5A. The Landsat 8-based temperature SD (Supplementary Fig. S4C) and kurtosis (Supplementary Fig. S4D) time series had patterns similar to the ones observed for the MODIS-based time series.

Seasonality in NDVI (Fig. 5B) and EVI (Fig. 5C) were opposite to the seasonality observed in temperature, as both vegetation indices decreased when temperature reached peak values. For the study period, MODIS-based NDVI values were higher than those observed for Landsat 8 and Sentinel 2 (Fig. 5B). Meanwhile, MODIS- and Landsat 8-based EVI values were very similar, and higher than values generated with Sentinel 2 images (Fig. 5C). Raw data for MODIS NDVI (Supplementary Fig. S5A) and EVI (Supplementary Fig. S5B), Landsat 8 NDVI (Supplementary Fig. S5C) and EVI (Supplementary Fig. S5D), Sentinel 2 NDVI (Supplementary Fig. S5E) and EVI (Supplementary Fig. S5F) also showed a marked seasonal pattern, where both indices decreased during weeks 1 to 16 of 2018, suggesting the seasonality was not an artifact of smoothing the time series.

3.3. Time series analysis

The inspection of the ACFs (Fig. 6A) and PACFs (Fig. 6B) suggested that *Ae aegypti*-borne arboviral cases and *Ae. aegypti* median egg counts followed first order seasonal autoregressive processes with a 3-week period. This means that observations, for both cases and egg counts, at any given time were associated with observations with a lag of one and three weeks. Using this information for these two variables, a null model with the following general form was fitted:

$$X_t = \mu + \varphi_1(X_{t-1} - \mu) + \varphi_3(X_{t-3} - \mu) - \varphi_1\varphi_3(X_{t-4} - \mu) + \varepsilon_t \quad (5)$$

This was then used to pre-whiten the covariate time series in order to select lags at which MODIS-based (Fig. 6C) and Landsat 8-based (Fig. 6D) variables were associated with arbovirus cases according to their CCFs. We used this information to build a full time series model for arboviral cases, which after a process of model selection by backward elimination (Table 1) resulted in a first-order seasonal autoregressive model. The selected model showed that number of cases had a nonlinear response to changes in MODIS-based temperature SD increasing 1 case for each 2 units of SD increase with a 4-week lag, while decreasing almost 1 case for each 2 units of MODIS-based SD increase with a 3-and 4-week lag and decreasing up to five cases for each Landsat 8 temperature SD unit increase with a 1-week lag. Arboviral cases increased around 4 cases for each 0.1 units of Landsat 8-based NDVI increase during the same week cases were recorded (Table 2). Arboviral cases were not significantly associated with the median, SD or kurtosis of *Ae. aegypti* egg counts (Supplementary Fig. S6A) nor with Sentinel 2-based NDVI and EVI (Supplementary Fig. S6B).

The CCFs of median number of *Ae. aegypti* eggs per ovitrap were not significantly associated with Sentinel 2-based NDVI and EVI (Supplementary Fig. S6C). In contrast, the median number of *Ae. aegypti* eggs per ovitrap was significantly associated with several MODIS-based (Fig. 6E) and Landsat 8-based (Fig. 6F) environmental variables presented in the full model in Table 3. After the process of model selection, the seasonal component was not significant (Table 3) and the median of eggs increased by approximately three units for each unit of MODIS-based temperature SD, while decreasing approximately 7 units for each 0.1 increase of Landsat 8-based NDVI, both variables having their impact on median egg number with a lag of 6 weeks (Table 4). The ACF (Supplementary Fig. S7A), PACF (Supplementary Fig. S7B) and CCFs with MODIS (Supplementary Fig. S7C) and Landsat 8 (Supplementary Fig. S7D) of the mean number of *Ae. aegypti* per ovitrap were similar to the ones observed for the median number of *Ae. aegypti* egg counts per ovitrap.

3.4. Synchrony

Aedes aegypti oviposition synchrony patterns are presented in Fig. 7A. Overall, oviposition synchrony was very low, with a regional synchrony of 0.04, which although statistically significant was very close to 0, i.e. a total lack of synchrony. The observed synchrony pattern is also

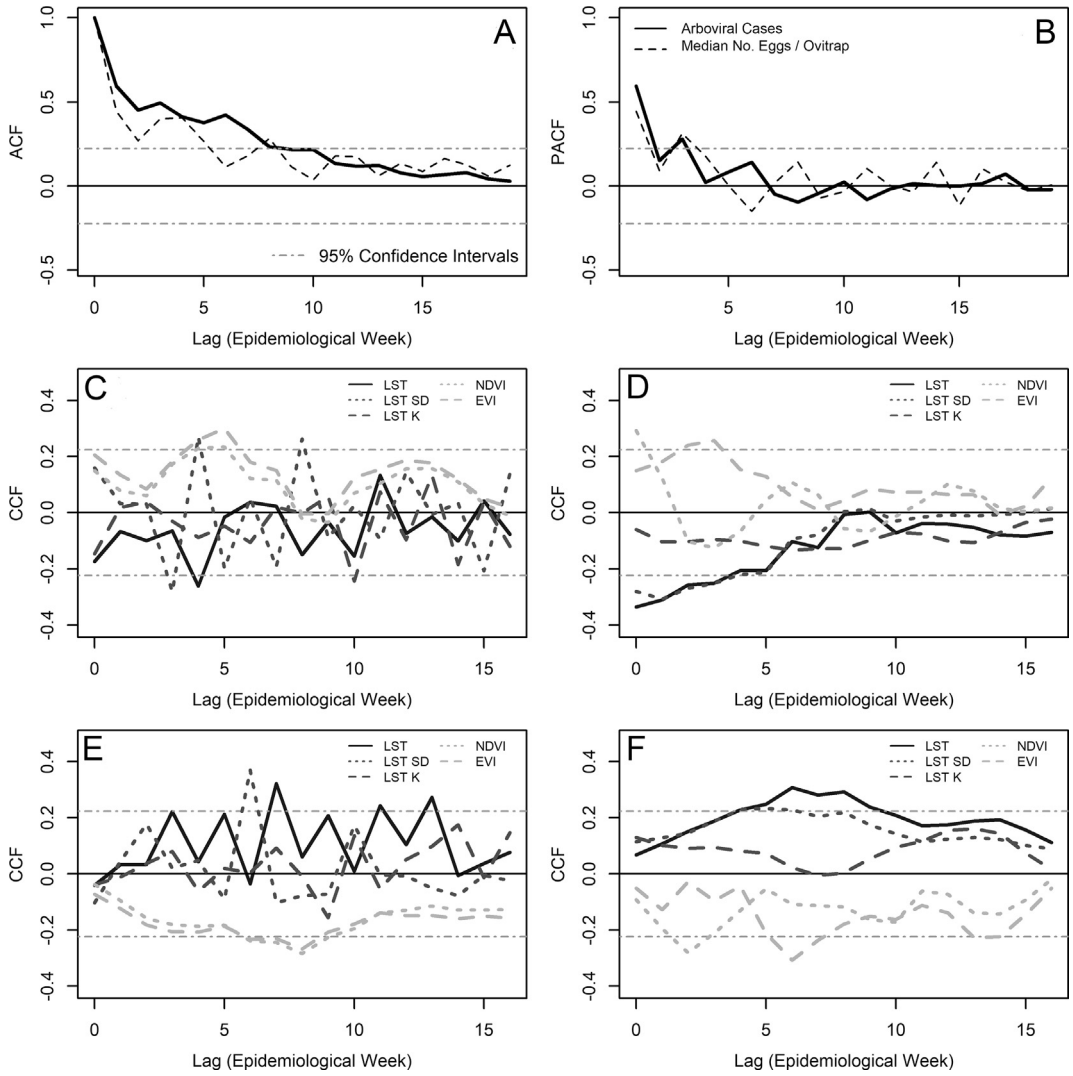

Fig. 6 Correlation functions. **A** Autocorrelation (ACF) and **B** partial autocorrelation function (PACF) for arboviral cases and median number, per ovitrap, of *Aedes aegypti* egg counts weekly time series. Lines are identified in the inset legend of panel **B. C** Cross-correlation function (CCF) between weekly arboviral cases and MODIS-based environmental variables, including land surface temperature, NDVI and EVI mean values, and also the standard deviation (SD) and kurtosis (K) of land surface temperature. **D** CCF between weekly arboviral cases and Landsat 8-based environmental variables, including land surface temperature, NDVI and EVI mean values, and also the SD and kurtosis of land surface temperature. **E** CCF between median *Ae. aegypti* egg counts and MODIS-based environmental variables, including land surface temperature, NDVI and EVI mean values, and also the SD and kurtosis (K) of land surface temperature. **F** CCF between median *Ae. aegypti* egg counts and Landsat 8-based environmental variables, including land surface temperature, NDVI and EVI mean values, and also the SD and kurtosis (K) of land surface temperature. In all panels the dot-dashed 95% confidence interval lines (see panel **A** for reference) indicate that correlations within the area are expected by chance. This means that peaks outside the 95% confidence interval lines are the time lags at which the number of arboviral cases (or median egg counts) was associated with itself in the ACF and PACF plots, or with the covariates in the CCF plots

suggestive of a travelling wave, as suggested by the 7 point estimates shown in Fig. 7A, where synchrony changes from positive to negative, around 400 m (where synchrony is significantly different from the regional estimate, as indicated by the black dot in Fig. 7A), suggesting patterns observed in Fig. 4B reflect a heterogeneous, or with dynamic spatiotemporal clusters, oviposition through time and space, also suggesting dynamic changes in the entomological exposure to *Ae. aegypti* in Puntarenas city. Landsat 8-based temperature (Fig. 7B) NDVI (Fig. 7C) and EVI (Fig. 7D) were significantly more synchronous than *Ae. aegypti* oviposition, with synchrony below 100 m being significantly higher than the regional values, suggesting these variables were not associated with *Ae. aegypti* oviposition in Puntarenas peninsula. Sentinel 2-based NDVI (Fig. 7E) synchrony significantly decreased at distances around 170 m when compared with the regional synchrony, while Sentinel 2-based EVI (Fig. 7F) had a pattern similar to the one observed for Landsat 8-based environmental variables with synchrony below 100 m being significantly higher than the regional values. Sentinel 2-based vegetation indices had low regional synchrony values similar to the ones observed for oviposition, suggesting oviposition synchrony might be driven by finely-grained environmental phenomena. For example, NDVI (Fig. 7E) decreased below the regional synchrony at distances of 170 m, the pattern most similar to what was observed for oviposition synchrony (Fig. 7A).

3.5. Spatial models

Selection for the best spatial model (Table 5) allowed us to identify Landsat 8-based EVI kurtosis and temperature as variables significantly associated with the mean number of *Ae. aegypti* eggs per ovitrap. The relationship with Landsat 8-based EVI kurtosis (*LEVIK*) was linear, with the number increasing by 3 eggs for each unit of kurtosis increase (Table 6), suggesting that leptokurtic vegetation changes were associated

Table 1
Model selection for the best time series model explaining counts of arbovirus cases at Puntarenas City, Costa Rica

Variables (Lag)	AIC
Null model: Autoregressive (1), Seasonal Autoregressive (3)	447.94
Full model: Autoregressive (1), Seasonal Autoregressive (3), MODIS-Temperature (4), MODIS-SD Temperature (3), MODIS-SD Temperature (4), MODIS-EVI (5), MODIS-NDVI (5), Landsat 8-Temperature (0), Landsat 8-SD temperature (1), Landsat 8-NDVI (0), Landsat 8-EVI (4)	436.08
Autoregressive (1), Seasonal Autoregressive (3), MODIS-SD Temperature (3), MODIS-SD Temperature (4), MODIS-EVI (5), MODIS-NDVI (5), Landsat 8-Temperature (0), Landsat 8-SD temperature (1), Landsat 8-NDVI (0), Landsat 8-EVI (4)	434.27
Autoregressive (1), Seasonal Autoregressive (3), MODIS-SD Temperature (3), MODIS-SD Temperature (4), MODIS-EVI (5), MODIS-NDVI (5), Landsat 8-Temperature (0), Landsat 8-SD temperature (1), Landsat 8-NDVI (0), Landsat 8-EVI (4)	432.52
Autoregressive (1), Seasonal Autoregressive (3), MODIS-SD Temperature (3), MODIS-SD Temperature (4), MODIS-EVI (5), Landsat 8-Temperature (0), Landsat 8-SD temperature (1), Landsat 8-NDVI (0), Landsat 8-EVI (4)	432.07
Autoregressive (1), Seasonal Autoregressive (3), MODIS-SD Temperature (3), MODIS-SD Temperature (4), MODIS-EVI (5), Landsat 8-Temperature (0), Landsat 8-SD temperature (1), Landsat 8-NDVI (0)	431.56
Autoregressive (1), Seasonal Autoregressive (3), MODIS-SD Temperature (3), MODIS-SD Temperature (4), Landsat 8-Temperature (0), Landsat 8-SD temperature (1), Landsat 8-NDVI (0)	**431.29**

Notes: AIC indicates the Akaike information criterion for each model. AIC is minimized by the best model, which is presented in bold. Lag indicates the time lag (in epidemiological weeks) for the correlation between arbovirus case number and the environmental variables considered.

with the oviposition of more eggs. However, the association with temperature (T) was nonlinear and we fitted a Gaussian generalized additive model described by the following equation:

$$Y_i = \mu + \beta LEVIK + s(T) + s(T, LEVIK) + \varepsilon_i \quad (6)$$

where $s(\ )$ denotes a smoothed function and parameters and assumptions were presented when defining Equation (4). The fitted surface is shown in Fig. 8, where it can be observed that the mean number of eggs increases with both T and $LEVIK$. The model surface shows that number of eggs increase at a rate of approximately 10 additional eggs for each °C above 36 °C, with temperature having a minimal impact on the mean number of *Ae. aegypti* eggs when below 36 °C. Finally, lack of significance for the Moran's I statistic (Table 6) supports that assumptions of spatial independence for the error were met, and therefore inferences for the model presented in Table 6 are valid.

4. Discussion

Our data analysis suggests that ovitrap counts are not useful to predict *Ae. aegypti*-borne arboviral cases at the studied site. This is interesting, given the general assumption that mosquito, and more generally vector abundance measurements, are useful to understand the risk for pathogen transmission (Smith et al., 2014), and evidence about associations between vector abundance and transmission at different spatial and temporal scales for dengue (Barrera et al., 2011; Cromwell et al., 2017; Parra et al., 2018; Li et al., 2019) and other vector-borne diseases (Chaves et al., 2011, 2014a; Poh et al., 2019). Among the diverse factors that may have influenced our results we think some might be related with *Ae. aegypti* ecology, as it is related to pathogen transmission, and some might be related to the predictability of events that are rare, or that occur at different spatial scales (Levin, 1992; Levins et al., 1994). To start, one of the reasons why egg counts might not be informative about disease transmission is related to the highly likely nonlinear association between egg abundance and adult mosquito abundance. The latter stage is responsible for pathogen transmission, but adult abundance might actually decrease with egg counts because of density-dependence, especially if the relationship is similar to what has been observed between adult and larval abundance (Wilson et al., 1990; Barrera et al., 2011; Chaves et al., 2012). Similarly, the productivity of *Ae. aegypti* changes across diverse container types (Schneider et al., 2004) and how adult mosquito productivity, i.e. the number of emerging adult mosquitoes, might ultimately reflect trade-offs in oviposition habitat selection by *Ae.*

Table 2
Parameter estimates for the best time series model explaining counts of arbovirus cases at Puntarenas City, Costa Rica

Parameter	Estimate ± SE
Mean	6.676 ± 6.166[a]
Autoregressive (1-week lag)	0.416 ± 0.107[a]
Seasonal autoregressive (3-weeks lag)	0.285 ± 0.114[a]
MODIS-based SD of temperature with 3-weeks lag	−0.468 ± 0.226[a]
MODIS-based SD of temperature with 4-weeks lag	0.488 ± 0.230[a]
Landsat 8-based SD of temperature with 1-week lag	−4.869 ± 1.766[a]
Landsat 8-based NDVI without a time lag	38.807 ± 15.426[a]
Variance error	10.46

Abbreviation: SE, standard error.
[a] Statistically significant ($P < 0.05$).

Table 3
Model selection for the best time series model explaining the median number of *Aedes aegypti* eggs per ovitrap at Puntarenas City, Costa Rica

Variables (Lag)	AIC
Null model: Autoregressive (1), Seasonal Autoregressive (3)	588.92
Full model: Autoregressive (1), Seasonal Autoregressive (3), MODIS-Temperature (7), MODIS-SD Temperature (6), MODIS-NDVI (8), MODIS-EVI (8), Landsat 8-Temperature (6), Landsat 8-SD Temperature (5), Landsat 8-NDVI (2), Landsat 8-EVI (6)	574.96
Autoregressive (1), Seasonal Autoregressive (3), MODIS-Temperature (7), MODIS-SD Temperature (6), MODIS-NDVI (8), MODIS-EVI (8), Landsat 8-Temperature (6), Landsat 8-NDVI (2), Landsat 8-EVI (6)	573.25
Autoregressive (1), Seasonal Autoregressive (3), MODIS-SD Temperature (6), MODIS-NDVI (8), MODIS-EVI (8), Landsat 8-Temperature (6), Landsat 8-NDVI (2), Landsat 8-EVI (6)	571.62
Autoregressive (1), Seasonal Autoregressive (3), MODIS-SD Temperature (6), MODIS-EVI (8), Landsat 8-Temperature (6), Landsat 8-NDVI (2), Landsat 8-EVI (6)	570.99
Autoregressive (1), Seasonal Autoregressive (3), MODIS-SD Temperature (6), Landsat 8-Temperature (6), Landsat 8-NDVI (2), Landsat 8-EVI (6)	570.03
Autoregressive (1), Seasonal Autoregressive (3), MODIS-SD Temperature (6), Landsat 8-Temperature (6), Landsat 8-EVI (6)	569.90
Autoregressive (1), Seasonal Autoregressive (3), MODIS-SD Temperature (6), Landsat 8-EVI (6)	**569.90**[a]
Autoregressive (1), MODIS-SD Temperature (6), Landsat 8-EVI (6)	571.18[a]

Notes: AIC indicates the Akaike information criterion for each model. AIC is minimized by the best model, which is presented in bold. Lag indicates the time lag (in epidemiological weeks) for the correlation between arbovirus case number and the environmental variables considered.
[a] Selected as best model due to the lack of a significant difference with the model minimizing AIC, through a Chi-square likelihood ratio test ($\chi^2 = 1.641$, $df = 1$, $P > 0.200$).

Table 4
Parameter estimates for the best time series model explaining the median number of *Aedes aegypti* eggs per ovitrap at Puntarenas City, Costa Rica

Parameter	Estimate ± SE
Mean	51.074 ± 10.775[a]
Autoregressive (1-week lag)	0.400 ± 0.107[a]
MODIS-based SD of temperature with 6-weeks lag	2.820 ± 0.609[a]
Landsat 8-based EVI with 6-weeks lag	−69.462 ± 19.297[a]
Variance error	65.02

Abbreviation: SE, standard error.
[a] Statistically significant ($P < 0.05$).

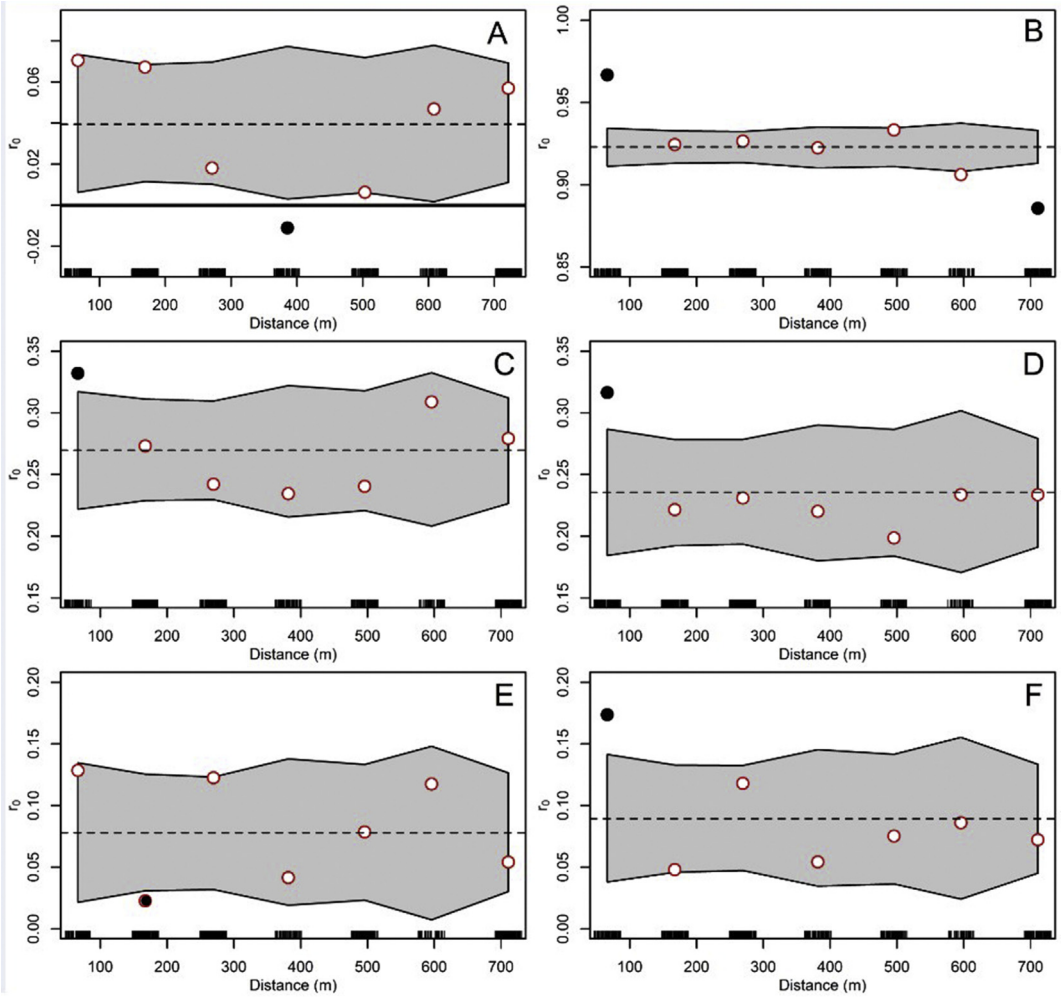

Fig. 7 Synchrony. **A** Weekly *Aedes aegypti* egg counts. **B** Landsat 8-based land surface temperature. **C** Landsat 8-based NDVI. **D** Landsat 8-based EVI. **E** Sentinel 2-based NDVI. **F** Sentinel 2-based EVI. Dots are average synchrony estimates for a given distance and the gray area indicates the 95% confidence intervals of the synchrony. For reference, the global (or average) synchrony (r_0) is presented as a black dashed line, and the black solid line indicates when synchrony is equal to zero. Filled circles represent synchrony estimates that are significantly different from the average synchrony ($P < 0.05$), while empty circles are not statistically different from the average synchrony estimate ($P > 0.05$)

aegypti (Harrington et al., 2008; Wong et al., 2012). The hypothesis of nonlinear abundance changes through the mosquito life-cycle has been supported by data fits to mathematical models looking at the abundance of *Ae. aegypti* (Chaves et al., 2012; Lana et al., 2014). More generally, ontogenetic niche shifts, such as those of mosquitoes that alternate between being aquatic and terrestrial organisms during their life-cycle, filter signals of density dependence that might be useful to predict population dynamics (Ripa & Ranta, 2007; Ranta et al., 2006; Ratikainen et al., 2008). Thus, not surprisingly, our results follow a pattern similar to what has been observed in data from other *Ae. aegypti* aquatic stages, where entomological indices based on the presence, or abundance, of either larvae or pupae, rarely correlate with dengue transmission (Bowman et al., 2014).

Mosquito eggs are not conspicuous life stages, which increases the ability to bias their counts. For example, accidently losing eggs during the manipulation of samples, might be a factor that could bias abundance estimates (Lenhart et al., 2005). The accidental loss of eggs is likely to occur when a large number of ovitraps are monitored by a mosquito surveillance crew with multiple responsibilities related to the management of vector-borne disease transmission (CENAPRECE, 2015; Tovar-Zamora et al., 2019). There is also the possibility that egg counts from ovitraps deployed over the larger area of Puntarenas could have been a better predictor for arboviral cases. However, within the Puntarenas peninsula it was clear that egg counts are highly variable at finely-grained spatial scales, and previous studies have shown this area to be the one with most persistent mosquito infestations (Marín Rodríguez & Díaz Ríos, 2012).

Nevertheless, the fact that temperature SD, a weather variable, had a significant impact on egg counts further supports that ovitraps are sensitive devices to estimate *Ae. aegypti* adult abundance, and most definitely to detect the presence of this important mosquito vector, as suggested by trials comparing multiple trap types (Resende et al., 2013; Codeço et al., 2015). For example, ovitraps had a higher sensitivity to detect *Ae. aegypti* than larval surveys (Nascimento et al., 2020). In this sense, the patterns observed in Costa Rica are similar to what has been observed for ovitraps in locations as diverse as Texas (Martin et al., 2019), Puerto Rico (Barrera et al., 2014), Brazil (Lana et al., 2014), Trinidad and Tobago (Chadee, 2009), México (Tovar-Zamora et al., 2019) and Argentina (Gimenez et al., 2020). These patterns also echo population dynamics patterns observed for adult mosquitoes, which are also sensitive to weather factors (Barrera et al., 2011; Ng et al., 2018; Scott et al., 2000). The relatively long delay of 6 weeks to see the impact of temperature and EVI might emerge *via* resonance, a phenomenon where natural populations cycles become amplified through a few generations in the presence of the right environmental conditions (Chaves et al., 2014b). For example, 6 weeks is an exact harmonic of the 3-week

Table 5
Model selection for the best spatial Gaussian generalized additive model explaining the median number of *Aedes aegypti* eggs per ovitrap at Puntarenas City, Costa Rica

Variables	AIC
Full model: LST, LNDVI, LEVI, SNDVI, SEVI, LSTSD, LNDVISD, LEVISD, SNDVISD, SEVISD, LSTK, LNDVIK, LEVIK, SNDVIK, SEVIK	566.91
LST, LNDVI, LEVI, SNDVI, SEVI, LSTSD, LNDVISD, LEVISD, SNDVISD, SEVISD, LSTK, LNDVIK, LEVIK, SEVIK	564.91
LST, LEVI, SNDVI, SEVI, LSTSD, LNDVISD, LEVISD, SNDVISD, SEVISD, LSTK, LNDVIK, LEVIK, SEVIK	562.91
LST, LEVI, SNDVI, SEVI, LSTSD, LNDVISD, LEVISD, SNDVISD, SEVISD, LSTK, LNDVIK, LEVIK	560.92
LST, SNDVI, SEVI, LSTSD, LNDVISD, LEVISD, SNDVISD, SEVISD, LSTK, LNDVIK, LEVIK	558.95
LST, SNDVI, SEVI, LSTSD, LNDVISD, SNDVISD, SEVISD, LSTK, LNDVIK, LEVIK	557.00
LST, SNDVI, SEVI, LSTSD, LNDVISD, SEVISD, LSTK, LNDVIK, LEVIK	555.10
LST, SEVI, LSTSD, LNDVISD, SEVISD, LSTK, LNDVIK, LEVIK	553.29
LST, SEVI, LSTSD, SEVISD, LSTK, LNDVIK, LEVIK	551.47
LST, SEVI, LSTSD, LSTK, LNDVIK, LEVIK	549.75
LST, LSTSD, LSTK, LNDVIK, LEVIK	547.93
LST, LSTSD, LNDVIK, LEVIK	546.31
LST, LSTSD, LEVIK	545.22
LST, LEVIK	**544.25**

Notes: AIC indicates the Akaike information criterion for each model. AIC is minimized by the best model, which is presented in bold. The following covariates were considered: Landsat 8-based temperature (LST); Landsat 8-based NDVI (LNDVI); Landsat 8-based EVI (LEVI); Sentinel 2-based NDVI (SNDVI); Sentinel 2-based EVI (SEVI); and also the SD and kurtosis of each of those variables which are indicated by adding, respectively, SD or K as suffix to the environmental variables.

Table 6
Parameter estimates for the best spatial Gaussian generalized additive model explaining the mean number of *Aedes aegypti* eggs per ovitrap at Puntarenas City, Costa Rica

Parameter	Estimate	SE	*t*-value	*P*-value
Intercept	12.290	1.869	6.575	5.22E-09[a]
Kurtosis of Landsat 8-based EVI (KEVI)	2.181	0.185	11.776	2.00E-16[a]
Moran's I	0.031			0.193
Approximate significance of smoothed terms				
Smoothed function	Estimate *df*	Residual *df*	*F*-value	*P*-value
s (Landsat 8 Temperature, LST)	1.866	2.354	4.323	0.0141[a]
s (LST, KEVI)	0.642	0.642	65.598	4.54E-09[a]

Abbreviation: *df*, degrees of freedom.
[a] Statistically significant ($P < 0.05$).

period of the seasonal component explaining median *Ae. aegypti* egg counts per ovitrap, the type of conditions enabling resonant increases in animal populations (Nisbet & Gurney, 1976). The best model explaining egg counts included EVI, a remotely sensed vegetation index that is associated with water in the environment (Pettorelli et al., 2005). EVI association with median egg counts was negative, probably reflecting that *Ae. aegypti* is primarily an artificial container species outside its native range in Africa (Dye, 1984; Wallace et al., 2018), needing water for the creation of its man-made larval habitats (Barrera et al., 1993; Predescu et al., 2006). However, *Ae. aegypti* larval habitats can be destroyed by an excess of rain, which can lead to a flushing of aquatic populations (Koenraadt & Harrington, 2008), ultimately reducing *Ae. aegypti* abundance (Scott et al., 2000). Still, the association is likely dynamic, as a previous, purely spatial study using high resolution satellite images for Puntarenas did not find an association between vegetation and *Ae. aegypti* abundance, which was more associated with the built urban environment (Fuller et al., 2010).

The travelling wave pattern of synchrony, where synchrony decreases with distance, and changes its sign before increasing back to its regional value (Ranta et al., 2006), to the best of our knowledge has been only reported for adults of *Armigeres subalbatus* (Coquillet), a common urban Aedini in Asia (Chaves, 2017b). This is an interesting pattern since it suggests that as much as human movement is an important factor for dengue transmission (Stoddard et al., 2009), vector movement might play a crucial role on *Ae. aegypti*-borne arboviral transmission. For example, vector control and *Ae. aegypti* dispersal ecology are prone to be asynchronous (Juarez et al., 2020). This asynchrony might ensure *Ae. aegypti* persistence in urban landscapes, as has been reported for both adult and larval *Ae albopictus* in Japan (Chaves, 2017b; Chaves et al., 2020b). Interestingly, although the pattern was not exactly the same, the synchrony of Sentinel 2-based NDVI also showed a significant decrease in synchrony at a shorter distance (170 m) than the one observed for *Ae. aegypti* eggs at 400 m. This pattern is suggestive of resonance in a two-dimensional expansion wave, a phenomenon, that to the best of our knowledge, has not been described in mosquitoes or other animal populations, but that has been described in neuron populations with hybrid synapses (Sun et al., 2013). Thus, the traveling wave pattern in *Ae. aegypti* egg count synchrony might emerge because of constrains in *Ae. aegypti* dispersal that might be conditioned, for example, by the availability of oviposition habitats (Edman et al., 1998), which in turn is linked with weather patterns (Juarez et al., 2020). This might reflect a process similar to the way neuron synapses are regulated in hybrid networks, those undergoing both chemical and electrical synapses (Sun et al., 2013). Interestingly, the evidence suggesting the emergence of this spatial pattern is further supported by the positive impact of high kurtosis, or leptokurtic, EVI on *Ae. aegypti* mean egg counts at the study site. This observation suggests that *Ae. aegypti* populations are likely to prefer less stable environments, as observed for treehole Aedini mosquitoes (Sota et al., 1994). This result also implies a nonlinear response to weather conditions, as mean egg numbers spatially increased with temperature in a fashion similar to what has been observed, temporally, for adult *Ae. aegypti* populations elsewhere (Chaves et al., 2012). For example, in Thailand, *Ae. aegypti* outbreaks, i.e. sudden changes in mosquito abundance, have been linked with the canalization of high temperatures into life history traits (Chaves et al., 2012, 2014b). More specifically, models have shown that prolonged high temperatures can reduce density-dependent mortality while simultaneously increasing fecundity and mosquito productivity (Chaves et al., 2014b).

Like mosquito egg counts, *Ae. aegypti*-borne arboviral case counts were associated with temperature SD, at multiple spatial scales. This result is in accordance with global observations for dengue, chikungunya and Zika (Wallace et al., 2018) where temperature has been shown as an important factor to explain time series of dengue cases across the globe (Stoddard et al., 2014; Chuang et al., 2017; Siraj et al., 2017; Oidtman et al., 2019). However, at the reduced spatial scale of this study we also found an impact for NDVI, a factor that has been reported as significant for dengue transmission dynamics at a country-wide scale in Costa Rica (Fuller et al., 2009) and Vietnam (Nguyen et al., 2020). This result might be related to the fact that vegetation growth is associated with several weather variables, like rainfall and temperature (Pettorelli et al., 2005). Finally, the fact that both egg and human cases were associated with temperature SD highlights the dependence of the system not only on average environmental conditions, but also on higher-order moments of environmental variability. This could emerge from Schmalhausen's law, the biological principle stating that organisms are sensitive to both the mean and the variability of the environment (Chaves, 2017a). Overall, our results also highlight the value of environmental information derived from satellite images for the surveillance of *Ae. aegypti* and the arboviruses it transmits, as documented in Southeast Asia (Nguyen et al., 2020). This pattern has also been observed for *Culex pipiens* L. and West Nile virus transmission in the USA (Chuang et al., 2012; Chuang & Wimberly, 2012; Poh et al., 2019); and *Anopheles albimanus* (Wiedemann) abundance and malaria infection in Mesoamerica (Hurtado et al., 2018a,b; Rejmankova et al., 1993; Rigg et al., 2019). Thus, our results are particularly important in the era of big data and unlimited computational

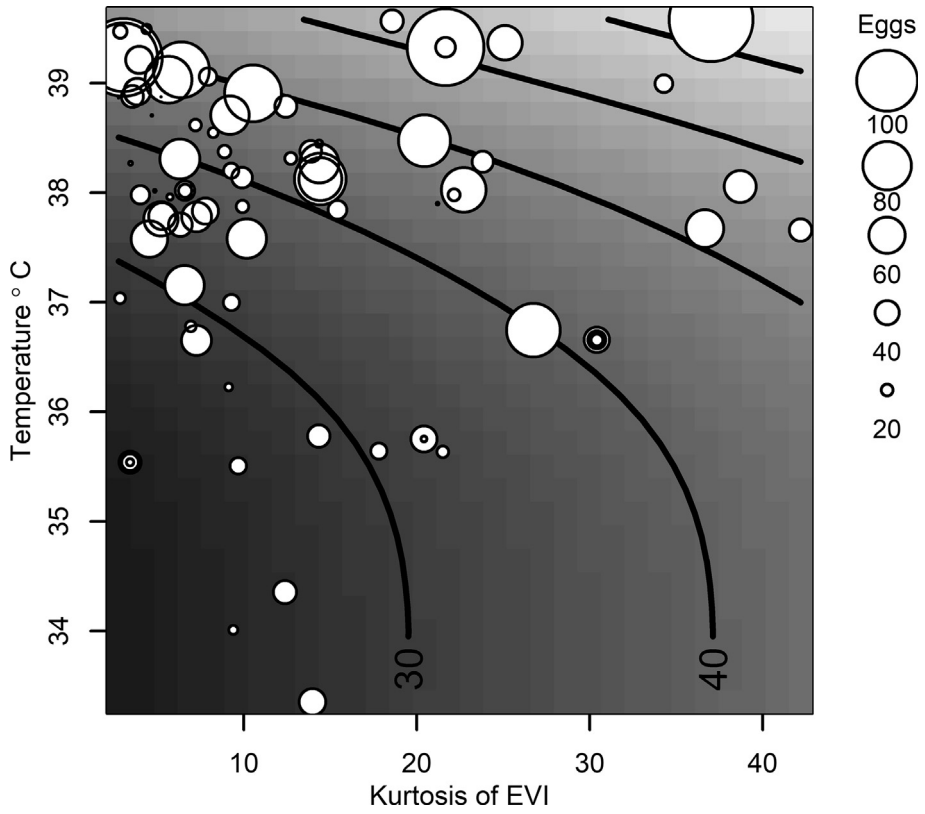

Fig. 8 Fitted surface from the best Gaussian generalized additive model explaining the mean number of *Aedes aegypti* egg counts per ovitrap as a function of Landsat 8-based EVI kurtosis and land surface temperature. Contour lines indicate the expected mean number of *Ae. aegypti* eggs per ovitrap. Contour lines were drawn in increasing values of 10 and observed values are represented by circles proportional to the mean number of eggs per ovitrap

power. Nowadays, satellite data can be streamlined into algorithms for vector-borne disease transmission forecasting and dynamic risk assessments.

Finally, ovitrap-based entomological surveillance might also help to guide vector control activities in sites with spatially heterogeneous and asynchronous changes in vector abundance, like these observed for *Ae. aegypti* in the present study. Major advantages of ovitrap use for *Ae. aegypti* surveillance include their low cost and ease for systematic field deployment and monitoring (CENAPRECE, 2015; Chaverri et al., 2018; Romero et al., 2019) and the potential involvement of local residents in vector surveillance efforts (Hamer et al., 2018; Tarter et al., 2019; Sousa et al., 2020). This study was carried out during a low transmission period for dengue in Costa Rica and the rest of the Americas in 2017 and 2018 (Perez et al., 2019). This low transmission prevented the use of mosquito control during our study, because mosquito control with pesticides in Costa Rica is only used for human disease outbreak management, and based on human case numbers (Vigilancia de la Salud, 2013). However, the Costa Rican national programme for integrated vector control management is currently evaluating the use of ovitraps to guide vector control in areas prone to dengue epidemics.

Ethical approval

This study was carried out in accordance with Article 7 from Law 9234 for biomedical research which grants the Epidemic Surveillance Division (Vigilancia de la Salud) of Costa Rica's Ministry of Health (Ministerio de Salud) the ability to perform activities with the dual goal of surveillance and research, which are exempted from the approval of an Institutional Research Board, as these efforts are deemed essential for health policy planning and decision making, and do not release individually identifiable data.

Data availability

Data are available upon reasonable request. The request needs to be accompanied by an appropriate ethical clearance in accordance with law 9234 for Biomedical Research in Costa Rica.

Declaration of competing interests

The authors confirm that there are no known conflicts of interest associated with this publication and that there has been no significant financial support for this work that could have influenced its outcome.

Funding

This study was funded by Costa Rica's Ministry of Health.

CRediT author statement

JAVC, EM, JMGA, GD, LFC and RMR designed the study. JAVC and RMR coordinated field sampling. GD, LMR, LFC, JMGA, EM, georeferenced ovitrap locations. GD and CAA verified all entomological data. LFC performed all tasks related with the remote sensing data processing and analysis. LFC made all maps. JAVC prepared Fig. 2. MRR, CAA and LMR compiled arboviral case data. LFC and GD analyzed the data. LFC, GD, MRR and LMR wrote the original draft of the manuscript. All authors read, edited and approved the final manuscript.

Acknowledgements

The authors thank the support from all members of the Programa Nacional de Manejo Integrado de Vectores – Región Pacífico Central for their help with this study. We are also very thankful to the residents of

Puntarenas that allowed us to place ovitraps in their households. This study benefited from discussions at PAHO sponsored entomo-virological surveillance meetings and from the generosity of the Mexican Government that donated the ovitraps and provided training for ovitrap use through the CENAPRECE. Finally, we thank Dr Sofia L. Ermida, Instituto Português do Mar e da Atmosfera (Lisbon, Portugal), for her advice to use scripts for processing Landsat 8 images using the Google Earth Engine, and Dr Mariel Dalmi Friberg Aponte, NASA Goddard Spatial Flight Center (Greenbelt, MD, USA), for her comments about satellite imagery and remote sensing.

Appendix A. Supplementary data

Supplementary data to this article can be found online at https://doi.org/10.1016/j.crpvbd.2021.100014.

References

Alfaro, A., 1921. Primera contribución al estudio de los zancudos de Costa Rica. Rev. Costa Rica 11, 239–246.
Arunachalam, N., Tana, S., Espino, F., Kittayapong, P., Abeyewickrem, W., Wai, K.T., et al., 2010. Eco-bio-social determinants of dengue vector breeding: A multicountry study in urban and periurban Asia. Bull. World Health Organ. 88, 173–184.
Baak-Baak, C.M., Cigarroa-Toledo, N., Arana-Guardia, R., Chim, W.A.C., Orilla, J.A.C., Machain-Williams, C., et al., 2016. Mosquito fauna associated with *Aedes aegypti* (Diptera: Culicidae) in Yucatán State of southeastern México, and checklist with new records. Florida Entomol. 99, 703–709.
Barrera, R., Acevedo, V., Felix, G.E., Hemme, R.R., Vazquez, J., Munoz, J.L., Amador, M., 2017. Impact of autocidal gravid ovitraps on chikungunya virus incidence in *Aedes aegypti* (Diptera: Culicidae) in areas with and without traps. J. Med. Entomol. 54, 387–395.
Barrera, R., Amador, M., Acevedo, V., Caban, B., Felix, G., Mackay, A.J., 2014. Use of the CDC autocidal gravid ovitrap to control and prevent outbreaks of *Aedes aegypti* (Diptera: Culicidae). J. Med. Entomol. 51, 145–154.
Barrera, R., Amador, M., MacKay, A.J., 2011. Population dynamics of *Aedes aegypti* and dengue as influenced by weather and human behavior in San Juan, Puerto Rico. PLoS Negl. Trop. Dis. 5, e1378.
Barrera, R., Avila, J., Gonzalez-Tellez, S., 1993. Unreliable supply of potable water and elevated *Aedes aegypti* larval indices - a casual relationship. J. Am. Mosq. Control Assoc. 9, 189–195.
Bisset, J.A., Marín, R., Rodríguez, M.M., Severson, D.W., Ricardo, Y., French, L., et al., 2013. Insecticide resistance in two *Aedes aegypti* (Diptera: Culicidae) strains from Costa Rica. J. Med. Entomol. 50, 352–361.
Bowman, L.R., Runge-Ranzinger, S., McCall, P.J., 2014. Assessing the relationship between vector indices and dengue transmission: A systematic review of the evidence. PLoS Negl. Trop. Dis. 8, e2848.
Brunsdon, C., Comber, L., 2015. An introduction to R for spatial analysis and mapping. Sage Publications LTD., London, p. 343.
Busetto, L., Ranghetti, L., 2016. MODIStsp: An R package for automatic preprocessing of MODIS Land Products time series. Comp. Geosci. 97, 40–48.
Calderón-Arguedas, O., Troyo, A., Solano, M.E., Avendaño, A., Beier, J.C., 2009. Urban mosquito species (Diptera: Culicidae) of dengue endemic communities in the greater Puntarenas area, Costa Rica. Rev. Biol. Trop. 57, 1223–1234.
Carvalho, G.C.d., Ceretti-Junior, W., Barrio-Nuevo, K.M., Wilk-da-Silva, R., Christe, R.O., Paula, M.B.d., et al., 2017. Composition and diversity of mosquitoes (Diptera: Culicidae) in urban parks in the South region of the city of São Paulo, Brazil. Biota Neotropica. 17, e20160274.
CENAPRECE, 2015. Guía metodológica para la vigilancia entomológica con ovitrampas. Secretaría de Salud. Subsecretaría de Prevención y Promoción de la Salud México, Ciudad de México, p. 33.
Ceretti-Júnior, W., Medeiros-Sousa, A.R., Multini, L.C., Urbinatti, P.R., Vendrami, D.P., Natal, D., et al., 2014. Immature mosquitoes in bamboo internodes in municipal parks, city of São Paulo, Brazil. J. Am. Mosq. Control Assoc. 30, 268–274.
Chadee, D.D., 2009. Oviposition strategies adopted by gravid *Aedes aegypti* (L.) (Diptera: Culicidae) as detected by ovitraps in Trinidad, west Indies (2002–2006). Acta Trop. 111, 279–283.
Chadee, D.D., Corbet, P.S., 1987. Seasonal incidence and diel patterns of oviposition in the field of the mosquito, *Aedes aegypti* (L.) (Diptera: Culicidae) in Trinidad, west Indies: A preliminary study. Ann. Trop. Med. Parasitol. 81, 151–161.
Chadee, D.D., Small, G.J., O'Malley, S.L., 1987. The description of the eggs of *Toxorhynchites moctezuma*. Mosq. Syst. 19, 237–242.
Chaverri, L.G., Dillenbeck, C., Lewis, D., Rivera, C., Romero, L.M., Chaves, L.F., 2018. Mosquito species (Diptera: Culicidae) diversity from ovitraps in a mesoamerican tropical rainforest. J. Med. Entomol. 55, 646–653.
Chaves, L.F., 2016. Globally invasive, withdrawing at home: *Aedes albopictus* and *Aedes japonicus* facing the rise of *Aedes flavopictus*. Int. J. Biometeorol. 60, 1727–1738.
Chaves, L.F., 2017a. Climate change and the biology of insect vectors of human pathogens. In: Johnson, S., Jones, H. (Eds.), Invertebrates and global climate change. Wiley, Chichester, UK, pp. 126–147.
Chaves, L.F., 2017b. Mosquito species (Diptera: Culicidae) persistence and synchrony across an urban altitudinal gradient. J. Med. Entomol. 54, 329–339.
Chaves, L.F., Calzada, J.E., Valderama, A., Saldaña, A., 2014. Cutaneous leishmaniasis and sand fly fluctuations are associated with El Niño in Panamá. PLoS Negl. Trop. Dis. 8, e3210.
Chaves, L.F., Cohen, J.M., Pascual, M., Wilson, M.L., 2008. Social exclusion modifies climate and deforestation impacts on a vector-borne disease. PLoS Negl. Trop. Dis. 2, e176.
Chaves, L.F., Friberg, M.D., 2021. *Aedes albopictus* and *Aedes flavopictus* (Diptera: Culicidae) pre-imaginal abundance patterns are associated with different environmental factors along an altitudinal gradient. Curr. Res. Insect Sci. 1, 100001.
Chaves, L.F., Friberg, M.D., Jian, J.-Y., Moji, K., 2019. Landscape and environmental factors influencing stage persistence and abundance of the bamboo mosquito, *Tripteroides bambusa* (Diptera: Culicidae), across an altitudinal gradient. Insects 10, 41.
Chaves, L.F., Friberg, M.D., Moji, K., 2020b. Synchrony of globally invasive *Aedes* spp. immature mosquitoes along an urban altitudinal gradient in their native range. Sci. Total Env. 734C, 139365.
Chaves, L.F., Hamer, G.L., Walker, E.D., Brown, W.M., Ruiz, M.O., Kitron, U.D., 2011. Climatic variability and landscape heterogeneity impact urban mosquito diversity and vector abundance and infection. Ecosphere 2, art70.
Chaves, L.F., Higa, Y., Lee, S.H., Jeong, J.Y., Heo, S.T., Kim, M., et al., 2013. Environmental forcing shapes regional house mosquito synchrony in a warming temperate island. Env. Entomol. 42, 605–613.
Chaves, L.F., Jian, J.-Y., Moji, K., 2018. Overwintering in the bamboo mosquito *Tripteroides bambusa* (Diptera: Culicidae) during a warm, but unpredictably changing, winter. Env. Entomol. 47, 148–158.
Chaves, L.F., Moji, K., 2018. Density dependence, landscape, and weather impacts on aquatic *Aedes japonicus japonicus* (Diptera: Culicidae) abundance along an urban altitudinal gradient. J. Med. Entomol. 55, 329–341.
Chaves, L.F., Morrison, A.C., Kitron, U.D., Scott, T.W., 2012. Nonlinear impacts of climatic variability on the density-dependent regulation of an insect vector of disease. Global Change Biol. 18, 457–468.
Chaves, L.F., Pascual, M., 2007. Comparing models for early warning systems of neglected tropical diseases. PLoS Negl. Trop. Dis. 1, e33.
Chaves, L.F., Ramírez Rojas, M., Prado, M., Garcés, J.L., Salas Peraza, D., Marín Rodríguez, R., 2020a. Health policy impacts on malaria transmission in Costa Rica. Parasitology 147, 999–1007.
Chaves, L.F., Scott, T.W., Morrison, A.C., Takada, T., 2014. Hot temperatures can force delayed mosquito outbreaks *via* sequential changes in *Aedes aegypti* demographic parameters in autocorrelated environments. Acta Trop. 129, 15–24.
Chen, S., Cordero, A., Bartels, J., 2017. Relatos del paisaje de Puntarenas. Siedin, San José.
Chuang, T.-W., Chaves, L.F., Chen, P.-J., 2017. Effects of local and regional climatic fluctuations on dengue outbreaks in southern Taiwan. Plos One 12, e0178698.
Chuang, T.-W., Henebry, G.M., Kimball, J.S., VanRoekel-Patton, D.L., Hildreth, M.B., Wimberly, M.C., 2012. Satellite microwave remote sensing for environmental modeling of mosquito population dynamics. Remote Sens. Env. 125, 147–156.
Chuang, T.W., Wimberly, M.C., 2012. Remote sensing of climatic anomalies and West Nile virus incidence in the northern Great Plains of the United States. Plos One 7, e46882.
Cleveland, W.S., Devlin, S.J., 1988. Locally weighted regression: An approach to regression analysis by local fitting. J. Am. Stat. Assoc. 83, 596–610.
Codeço, C.T., Lima, A.W.S., Araújo, S.C., Lima, J.B.P., Maciel-de-Freitas, R., Honório, N.A., et al., 2015. Surveillance of *Aedes aegypti:* Comparison of house index with four alternative traps. PLoS Negl. Trop. Dis. 9, e0003475.
Colón-González, F.J., Peres, C.A., Steiner São Bernardo, C., Hunter, P.R., Lake, I.R., 2017. After the epidemic: Zika virus projections for Latin America and the Caribbean. PLoS Negl. Trop. Dis. 11, e0006007.
Cromwell, E.A., Stoddard, S.T., Barker, C.M., Van Rie, A., Messer, W.B., Meshnick, S.R., et al., 2017. The relationship between entomological indicators of *Aedes aegypti* abundance and dengue virus infection. PLoS Negl. Trop. Dis. 11, e0005429.
Day, J.F., 2016. Mosquito oviposition behavior and vector control. Insects 7, 65.
de la Salud, Vigilancia, 2013. Lineamientos para el Control y prevención del Dengue. Ministerio de Salud, San Jose, Costa Rica, p. 42.
de la Salud, Vigilancia, 2019. In: Marin Rodriguez, R. (Ed.), Boletín epidemiológico No. 20. Ministerio de Salud de Costa Rica, San José, p. 15.
Didan, K., 2015a. MOD13Q1 MODIS/Terra vegetation indices 16-day L3 global 250 m SIN grid V006 [data set]. NASA EOSDIS land processes DAAC. https://doi.org/10.5067/MODIS/MOD13Q1.006. (Accessed 8 October 2018).
Didan, K., 2015b. MYD13Q1 MODIS/Aqua vegetation indices 16-day L3 global 250 m SIN grid V006 [data set]. LP DAAC - MOD13Q1 (usgs.gov). (Accessed 8 October 2018).
Drusch, M., Del Bello, U., Carlier, S., Colin, O., Fernandez, V., Gascon, F., et al., 2012. Sentinel-2: ESA's optical high-resolution mission for GMES operational services. Remote Sens. Env. 120, 25–36.
Dye, C., 1984. Models for the population dynamics of the yellow fever mosquito, *Aedes aegypti*. J. Anim. Ecol. 53, 247–268.
Edman, J.D., Scott, T.W., Costero, A., Morrison, A.C., Harrington, L.C., Clark, G.G., 1998. *Aedes aegypti* (Diptera: Culicidae) movement influenced by availability of oviposition sites. J. Med. Entomol. 35, 578–583.
Ermida, S.L., Soares, P., Mantas, V., Göttsche, F.-M., Trigo, I.F., 2020. Google Earth engine open-source code for land surface temperature estimation from the Landsat series. Remote Sens. 12, 1471.
ESA, 2015. Sentinel-2 user handbook. European Space Agency, Paris, France, p. 64.
Faraway, J.J., 2004. Linear models with R. CRC Press, Boca Raton.
Faraway, J.J., 2006. Extending the linear model with R: Generalized linear, mixed effects and nonparametric regression models. CRC Press, Boca Raton.
Fernández-Salas, I., Danis-Lozano, R., Casas-Martínez, M., Ulloa, A., Bond, J.G., Marina, C.F., et al., 2015. Historical inability to control *Aedes aegypti* as a main contributor of fast dispersal of chikungunya outbreaks in Latin America. Antiviral Res. 124, 30–42.

Fuller, D.O., Troyo, A., Beier, J.C., 2009. El Niño Southern Oscillation and vegetation dynamics as predictors of dengue fever cases in Costa Rica. Env. Res. Lett. 4, 140111–140118.
Fuller, D.O., Troyo, A., Calderon-Arguedas, O., Beier, J.C., 2010. Dengue vector (*Aedes aegypti*) larval habitats in an urban environment of Costa Rica analysed with ASTER and QuickBird imagery. Int. J. Remote Sensing 31, 3–11.
Futami, K., Valderrama, A., Baldi, M., Minakawa, N., Marín Rodríguez, R., Chaves, L.F., 2015. New and common haplotypes shape genetic diversity in Asian tiger mosquito populations from Costa Rica and Panamá. J. Econ. Entomol. 108, 761–768.
Gimenez, J.O., Alvarez, C.N., Almirón, W.R., Stein, M., 2020. Meteorological variables associated with the temporal oviposition rate of *Aedes aegypti* (Diptera: Culicidae) in resistencia city, Chaco Province, northeastern Argentina. Acta Trop. 212, 105678.
González Elizondo, M., 2018. Informe de vigilancia de Arbovirus basada en laboratorio. Tres Ríos, Centro Nacional de Referencia de Virología - INCIENSA, p. 18.
Google, 2020. Earth engine data Catalog. https://developers.google.com/earth-engine/datasets. (Accessed 1 November 2020).
Gouhier, T.C., Guichard, F., 2014. Synchrony: Quantifying variability in space and time. Methods Ecol. Evol. 5, 524–533.
Gubler, D.J., 1989. *Aedes aegypti* and *Aedes aegypti*-borne disease control in the 1990s: Top down or bottom up. Am. J. Trop. Med. Hyg. 40, 571–578.
Hamer, S.A., Curtis-Robles, R., Hamer, G.L., 2018. Contributions of citizen scientists to arthropod vector data in the age of digital epidemiology. Curr. Opinion Insect Sci. 28, 98–104.
Harbach, R., Knight, K., 1978. A mosquito taxonomic glossary. XV. The Egg. Mosq. Syst. 10, 249–298.
Harrington, L.C., Ponlawat, A., Edman, J.D., Scott, T.W., Vermeylen, F., 2008. Influence of container size, location, and time of day on oviposition patterns of the dengue vector, *Aedes aegypti*, in Thailand. Vector-Borne Zoon. Dis. 8, 415–423.
Hoshi, T., Higa, Y., Chaves, L.F., 2014. *Uranotaenia novobscura ryukyuana* (Diptera: Culicidae) population dynamics are denso-dependent and autonomous from weather fluctuations. Ann. Entomol. Soc. Am. 107, 136–142.
Hoshi, T., Imanishi, N., Moji, K., Chaves, L.F., 2017. Density dependence in a seasonal time series of the bamboo mosquito, *Tripteroides bambusa* (Diptera: Culicidae). Canadian Entomol. 149, 338–344.
Hurtado, L.A., Calzada, J.E., Rigg, C.A., Castillo, M., Chaves, L.F., 2018a. Climatic fluctuations and malaria transmission dynamics, prior to elimination, in Guna Yala, República de Panamá. Malaria J. 17, 85.
Hurtado, L.A., Rigg, C.A., Calzada, J.E., Dutary, S., Bernal, D., Koo, S.I., Chaves, L.F., 2018b. Population dynamics of *Anopheles albimanus* (Diptera: Culicidae) at Ipetí-guna, a village in a region targeted for malaria elimination in Panamá. Insects 9, 164.
INEC, 2012. X censo nacional de Población y VI de Vivienda 2011: Resultados generales. Instituto Nacional de Estadísticas y Censos, San José, p. 142.
Johansson, M.A., Cummings, D.A., Glass, G.E., 2009. Multiyear climate variability and dengue - el Niño Southern Oscillation, weather, and dengue incidence in Puerto Rico, Mexico, and Thailand: A longitudinal data analysis. PLoS Med. 6, e1000168.
Juarez, J.G., Garcia-Luna, S., Chaves, L.F., Carbajal, E., Valdez, E., Avila, C., et al., 2020. Dispersal of female and male *Aedes aegypti* from discarded container habitats using a stable isotope mark-capture study design in South Texas. Sci. Rep. 10, 6803.
Kitron, U., Otieno, L., Hungerford, L., Odulaja, A., Brigham, W., Okello, O., et al., 1996. Spatial analysis of the distribution of tsetse flies in the Lambwe Valley, Kenya, using Landsat TM satellite imagery and GIS. J. Animal Ecol. 65, 371–380.
Koenraadt, C.J.M., Harrington, L.C., 2008. Flushing effect of rain on container-inhabiting mosquitoes *Aedes aegypti* and *Culex pipiens* (Diptera: Culicidae). J. Med. Entomol. 45, 28–35.
Kumm, H.W., Komp, W.H.W., Ruiz, H., 1940. The mosquitoes of Costa Rica. Am. J. Trop. Med. Hyg. 1, 385–422.
Lana, R.M., Carneiro, T.G.S., Honório, N.A., Codeço, C.T., 2014. Seasonal and nonseasonal dynamics of *Aedes aegypti* in Rio de Janeiro, Brazil: Fitting mathematical models to trap data. Acta. Trop. 129, 25–32.
Lee-Lui, M., Alfaro-Alvarado, J., Quesada-Johnson, A., Taylor-Castillo, L., Hun-Opfer, L., 2008. Prevalencia de anticuerpos contra virus dengue en el cantón de Golfito (2005) y en el Distrito Central de Puntarenas (2005–2006), Costa Rica. Acta Méd Costarricense 50, 147–152.
Lenhart, A.E., Walle, M., Cedillo, H., Kroeger, A., 2005. Building a better ovitrap for detecting *Aedes aegypti* oviposition. Acta Trop. 96, 56–59.
Levin, S., 1992. The problem of scale and pattern in ecology. Ecology 73, 1943–1967.
Levins, R., Awerbuch, T., Brinkmann, U., Eckardt, I., Epstein, P., Makhoul, N., et al., 1994. The emergence of new diseases. Am. Sci. 82, 52–60.
Li, R., Xu, L., Bjørnstad, O.N., Liu, K., Song, T., Chen, A., et al., 2019. Climate-driven variation in mosquito density predicts the spatiotemporal dynamics of dengue. Proc. Natl. Acad. Sci. USA 116, 3624–3629.
Marín Mena, L., 2007. Desinfección del agua: Sistemas utilizados en AyA. Hydrogenesis 5, 35–46.
Marín Rodríguez, R., Díaz Ríos, M., 2012. Sitios de cría del *Aedes aegypti* en la Región Pacífico Central de Costa Rica. Rev. Costarricense Salud Públ. 21, 81–86.
Martin, E., Medeiros, M.C., Carbajal, E., Valdez, E., Juarez, J.G., Garcia-Luna, S., et al., 2019. Surveillance of *Aedes aegypti* indoors and outdoors using Autocidal Gravid Ovitraps in South Texas during local transmission of Zika virus, 2016 to 2018. Acta Trop. 192, 129–137.
Mena, N., Troyo, A., Bonilla-Carrión, R., Calderón-Arguedas, Ó., 2011. Factores asociados con la incidencia de dengue en Costa Rica. Rev Panamericana Salud Públ. 29, 234–242.
NASA, 2018. NASA Land Processes Distributed Active Archive Cente. https://lpdaac.usgs.gov. (Accessed 8 November 2020).
Nascimento, K.L.C., Silva, J.F.M.d., Zequi, J.A.C., Lopes, J., 2020. Comparison between Larval Survey Index and Positive Ovitrap Index in the evaluation of populations of *Aedes* (*Stegomyia*) *aegypti* (Linnaeus, 1762) North of Paraná. Brazil. Env. Health Insights 14.
Ng, K.-C., Chaves, L.F., Tsai, K.-H., Chuang, T.-W., 2018. Increased adult *Aedes aegypti* and *Culex quinquefasciatus* (Diptera: Culicidae) abundance in a dengue transmission hotspot, compared to a coldspot, within Kaohsiung city, Taiwan. Insects 9, 98.
Nguyen, L.T., Le, H.X., Nguyen, D.T., Ho, H.Q., Chuang, T.W., 2020. Impact of climate variability and abundance of mosquitoes on dengue transmission in Central Vietnam. Int. J. Env. Res. Public Health 17, 2453.
Nisbet, R.M., Gurney, W.S.C., 1976. Population dynamics in a periodically varying environment. J. Theor. Biol. 56, 459–475.
Oidtman, R.J., Lai, S., Huang, Z., Yang, J., Siraj, A.S., Reiner, R.C., et al., 2019. Inter-annual variation in seasonal dengue epidemics driven by multiple interacting factors in Guangzhou, China. Nat. Com. 10, 1148.
Ortega-Morales, A.I., Moreno-García, M., González-Acosta, C., Correa-Morales, F., 2018. Mosquito surveillance in Mexico: The use of ovitraps for *Aedes aegypti, Ae. albopictus*, and non-target species. Florida Entomol. 101, 623–626.
PAHO, 2017. Seguimiento de la Estrategia de Gestión Integrada para la prevención y el control del dengue en el marco de transición hacia el manejo integrado de las Arbovirosis. Ciudad de Panamá, p. 78.
Parra, M.C.P., Fávaro, E.A., Dibo, M.R., Mondini, A., Eiras, Á.E., Kroon, E.G., et al., 2018. Using adult *Aedes aegypti* females to predict areas at risk for dengue transmission: A spatial case-control study. Acta Trop. 182, 43–53.
Perez, F., Llau, A., Gutierrez, G., Bezerra, H., Coelho, G., Ault, S., et al., 2019. The decline of dengue in the Americas in 2017: Discussion of multiple hypotheses. Trop. Med. Int. Health 24, 442–453.
Pettorelli, N., Vik, J.O., Mysterud, A., Gaillard, J.-M., Tucker, C.J., Stenseth, N.C., 2005. Using the satellite-derived NDVI to assess ecological responses to environmental change. Trends Ecol. Evol. 20, 503–510.
Poh, K.C., Chaves, L.F., Reyna-Nava, M., Roberts, C.M., Fredregill, C., Bueno, R., Debboun, M., Hamer, G.L., 2019. The influence of weather and weather variability on mosquito abundance and infection with West Nile virus in Harris County, Texas, USA. Sci. Total Env. 675, 260–272.
Predescu, M., Levins, R., Awerbuch-Friedlander, T., 2006. Analysis of a nonlinear system for community intervention in mosquito control. Dis. Continuous Dynamical Syst. Ser. B 6, 605–622.
Priestley, M.B., 1988. Non-linear and non-stationary time series analysis. Academic Press, London.
Ranta, E., Lundberg, P., Kaitala, V., 2006. Ecology of populations. Cambridge University Press, Cambridge.
Ratikainen, I.I., Gill, J.A., Gunnarsson, T.G., Sutherland, W.J., Kokko, H., 2008. When density dependence is not instantaneous: Theoretical developments and management implications. Ecol. Lett. 11, 184–198.
Regis, L., Monteiro, A.M., de Melo-Santos, M.A.V., Silveira, J.C., Furtado, A.F., Acioli, R.V., et al., 2008. Developing new approaches for detecting and preventing *Aedes aegypti* population outbreaks: Basis for surveillance, alert and control system. Mem. Inst. Oswaldo Cruz 103, 50–59.
Reinhold, J.M., Lazzari, C.R., Lahondère, C., 2018. Effects of the environmental temperature on *Aedes aegypti* and *Aedes albopictus* mosquitoes: A review. Insects 9, 158.
Rejmankova, E., Roberts, D., Harbach, R., Pecor, J., Peyton, E., Manguin, S., et al., 1993. Environmental and regional determinants of *Anopheles* (Diptera: Culicidae) larval distribution in Belize, Central America. Env. Entomol. 22, 978–992.
Resende, M.C.d., Silva, I.M., Ellis, B.R., Eiras, A.E., 2013. A comparison of larval, ovitrap and MosquiTRAP surveillance for *Aedes (Stegomyia) aegypti*. Mem. Inst. Oswaldo Cruz 108, 1024–1030.
Rigg, C.A., Hurtado, L.A., Calzada, J.E., Chaves, L.F., 2019. Malaria infection rates in *Anopheles albimanus* (Diptera: Culicidae) at Ipetí-guna, a village within a region targeted for malaria elimination in Panamá. Inf. Genet. Evol. 69, 216–223.
Ripa, J., Ranta, E., 2007. Biological filtering of correlated environments: Towards a generalised Moran theorem. Oikos 116, 783–792.
Ritchie, S.A., Long, S., Hart, A., Webb, C.E., Russell, R.C., 2003. An adulticidal sticky ovitrap for sampling container-breeding mosquitoes. J. Am. Mosq. Control Assoc. 19, 235–242.
Ritchie, S.A., Long, S., Smith, G., Pyke, A., Knox, T.B., 2004. Entomological investigations in a focus of dengue transmission in Cairns, Queensland, Australia, by using the sticky ovitraps. J. Med. Entomol. 41, 1–4.
Romero, L.M., Chaverri, L.G., Chaves, L.F., 2019. Mosquito (Diptera: Culicidae) species composition in ovitraps from a mesoamerican tropical montane cloud forest. J. Med. Entomol. 56, 491–500.
Sáenz, E., González, L., Viquez, M., Lara, J., de los Angeles Valverde, M., 1999. Circulación del virus dengue 3 en Costa Rica, 1994-1997. Acta Méd. Costarricense 41, 24–31.
San Martín, J.L., Brathwaite, O., Zambrano, B., Solórzano, J.O., Bouckenooghe, A., Dayan, G.H., Guzmán, M.G., 2010. The epidemiology of dengue in the Americas over the last three decades: A worrisome reality. Am. J. Trop. Med. Hyg. 82, 128–135.
Santos Neto, L.G.d., Azevedo Marques, C.C.d., 1996. Sobre alguns ovos de mosquitos (Diptera, Culicidae) que colonizam recipients artificiais. Rev. Bras. Entomol. 40, 17–20.
Schneider, J.R., Morrison, A.C., Astete, H., Scott, T.W., Wilson, M.L., 2004. Adult size and distribution of *Aedes aegypti* (Diptera : Culicidae) associated with larval habitats in Iquitos, Peru. J. Med. Entomol. 41, 634–642.
Scott, T.W., Morrison, A.C., Lorenz, L.H., Clark, G.G., Strickman, D., Kittayapong, P., et al., 2000. Longitudinal studies of *Aedes aegypti* (Diptera: Culicidae) in Thailand and Puerto Rico: Population dynamics. J. Med. Entomol. 37, 77–88.
Serre, P.A., 1921. Insectes piquants et parasites au Costa Rica. Bull. Mus. Nat. Hist. Nat. 27, 170–172.

Shumway, R.H., Stoffer, D.S., 2011. Time series analysis and its applications, 3rd ed. Springer, New York, p. 572.
Siraj, A.S., Oidtman, R.J., Huber, J.H., Kraemer, M.U.G., Brady, O.J., Johansson, M.A., Perkins, T.A., 2017. Temperature modulates dengue virus epidemic growth rates through its effects on reproduction numbers and generation intervals. PLoS Negl. Trop. Dis. 11, e0005797.
Smith, D.L., Perkins, T.A., Reiner, J.R.C., Barker, C.M., Niu, T., Chaves, L.F., et al., 2014. Recasting the theory of mosquito-borne pathogen transmission dynamics and control. Trans. Roy. Soc. Trop. Med. Hyg. 108, 185–197.
Soper, F.L., 1967. Dynamics of *Aedes aegypti* distribution and density. Seasonal fluctuations in the Americas. Bull. World Health Organ. 36, 536–538.
Sota, T., Mogi, M., Hayamizu, E., 1994. Habitat stability and the larval mosquito community in treeholes and other containers on a temperate island. Res. Pop. Ecol. 36, 93–104.
Soto-Garita, C., Tsomogyi, T., Vicente-Santos, A., Corrales-Aguilar, E., 2016. Molecular characterization of two major dengue outbreaks in Costa Rica. Am. J. Trop. Med. Hyg. 95, 201–205.
Sousa, L.B., Fricker, S.R., Doherty, S.S., Webb, C.E., Baldock, K.L., Williams, C.R., 2020. Citizen science and smartphone e-entomology enables low-cost upscaling of mosquito surveillance. Sci. Total Env. 704, 135349.
Stearns, S.C., 1981. On measuring fluctuating environments - predictability, constancy, and contingency. Ecology 62, 185–199.
Stoddard, S.T., Morrison, A.C., Vazquez-Prokopec, G.M., Soldan, V.P., Kochel, T.J., Kitron, U., et al., 2009. The role of human movement in the transmission of vector-borne pathogens. PLoS Negl. Trop. Dis. 3.
Stoddard, S.T., Wearing, H.J., Reiner Jr., R.C., Morrison, A.C., Astete, H., Vilcarromero, S., et al., 2014. Long-term and seasonal dynamics of dengue in Iquitos, Peru. PLoS Negl. Trop. Dis. 8, e3003.
Sun, J., Deng, B., Liu, C., Yu, H., Wang, J., Wei, X., Zhao, J., 2013. Vibrational resonance in neuron populations with hybrid synapses. Appl. Math. Modelling 37, 6311–6324.
Tarter, K.D., Levy, C.E., Yaglom, H.D., Adams, L.E., Plante, L., Casal, M.G., et al., 2019. Using citizen science to enhance surveillance of *Aedes aegypti* in Arizona, 2015–17. J. Am. Mosq. Control Assoc. 35, 11.
Tovar-Zamora, I., Caraveo-Patiño, J., Penilla-Navarro, R.P., Serrano-Pinto, V., Méndez-Galván, J., Martínez, A.M., et al., 2019. Seasonal variation in abundance of dengue vector in the southern part of the Baja California Peninsula, Mexico. Southwestern Entomol. 44, 885–895.
Troyo, A., Fuller, D.O., Calderón-Arguedas, O., Solano, M.E., Beier, J.C., 2009. Urban structure and dengue fever in Puntarenas, Costa Rica. Singapore J. Trop. Geogr. 30, 265–282.
USNPS, 2020. Data Sources & Accuracy for National Park Service Maps. https://www.nps.gov/hfc/carto/data-sources.cfm. (Accessed 31 August 2020).
Vargas, M., 1961. Algunas observaciones sobre los hábitos de *Anopheles* (*N.*) *albimanus* y *Anopheles* (*A.*) *punctimacula* adultos, en la localidad de Matapalo (Puntarenas) Costa Rica. Rev. Biol. Trop. 9, 153–170.
Venables, W.N., Ripley, B.D., 2002. Modern applied statistics with S. Springer, New York.
Vermote, E., Justice, C., Claverie, M., Franch, B., 2016. Preliminary analysis of the performance of the Landsat 8/OLI land surface reflectance product. Remote Sensing Env. 185, 46–56.
Villanueva, J.B., 2009. Caracterización por sector productivo de las empresas de la subregión del Gran Puntarenas, Costa Rica (2006). InterSedes: Rev. Sedes Regionales 10, 1–21.
Wallace, R., Chaves, L.F., Bergmann, L., Ayres Lopes, C.f.J., Hogerwerf, L., Kock, R., Wallace, R.G., 2018. Clear-cutting disease control: Capital-led deforestation, public health austerity, and vector-borne infection. Springer, New York.
Wan, Z., Hook, S., Hulley, G., 2015. MOD11A1 MODIS/Terra Land Surface Temperature/Emissivity Daily L3 Global 1 km SIN Grid V006. 2015, distributed by NASA EOSDIS Land Processes DAAC. https://doi.org/10.5067/MODIS/MOD11A1.006. (Accessed 29 August 2020).
Weaver, S.C., Charlier, C., Vasilakis, N., Lecuit, M., 2018. Zika, chikungunya, and other emerging vector-borne viral diseases. Ann. Rev. Med. 69, 395–408.
Weaver, S.C., Costa, F., Garcia-Blanco, M.A., Ko, A.I., Ribeiro, G.S., Saade, G., et al., 2016. Zika virus: History, emergence, biology, and prospects for control. Antiviral Res. 130, 69–80.
Weaver, S.C., Reisen, W.K., 2010. Present and future arboviral threats. Antiviral Res. 85, 328–345.
Wilson, M.L., Agudelo-Silva, F., Spielman, A., 1990. Increased abundance, size, and longevity of food-deprived mosquito populations exposed to a fungal larvicide. Am. J. Trop. Med. Hyg. 43, 551–556.
Wong, J., Morrison, A.C., Stoddard, S.T., Astete, H., Chu, Y.Y., Baseer, I., Scott, T.W., 2012. Linking oviposition site choice to offspring fitness in *Aedes aegypti*: Consequences for targeted larval control of dengue vectors. PLoS Negl. Trop. Dis. 6, e1632.
World Meteorological Organization, 2020. World weather information Service: Puntarenas. https://worldweather.wmo.int/en/city.html?cityId=1128. (Accessed 29 August 2020).
Yactayo, S., Staples, J.E., Millot, V., Cibrelus, L., Ramon-Pardo, P., 2016. Epidemiology of chikungunya in the Americas. J. Inf. Dis. 214, S441–S445.
Zar, J.H., 1998. Biostatistical analysis. Prentice Hall, San Francisco.
Zardkoohi, A., Castañeda, D., Lol, J.C., Castillo, C., Lopez, F., Marín Rodriguez, R., Padilla, N., 2020. Co-occurrence of kdr mutations V1016I and F1534C and its association with phenotypic resistance to pyrethroids in *Aedes aegypti* (Diptera: Culicidae) populations from Costa Rica. J. Med. Entomol. 57, 830–836.